

Aus der Klinik für Kardiologie, Pneumologie und Angiologie
der Heinrich-Heine-Universität Düsseldorf
Direktor der Klinik: Prof. Dr. med. Malte Kelm

Influence of Nuclear-factor-erythroid-2-related-factor 2 (Nrf2)
on left ventricular and coronary function

Dissertation

zur Erlangung des Grades eines Doktors der Medizin der Medizinischen
Fakultät der Heinrich-Heine-Universität Düsseldorf

vorgelegt von

Mathias Weidenbach

2018

Als Inauguraldissertation gedruckt mit der Genehmigung der Medizinischen
Fakultät der Heinrich-Heine-Universität Düsseldorf

Gez.:

Dekan: Prof. Dr. med. Nikolaj Klöcker

Erstgutachterin: Prof. Dr. rer. nat. Miriam M. Cortese-Krott

Zweitgutachter: Prof. Dr. rer. nat. Christoph V. Suschek

Tag der mündlichen Prüfung: 19.06.2018

Teile dieser Arbeit wurden veröffentlicht [1]:

Erkens, R; Kramer, C M; Luckstadt, W; Panknin, C; Krause, L; Weidenbach, M; Dirzka, J; Krenz, T; Mergia, E; Suvorava, T; Kelm, M; Cortese-Krott, M M., (2015) Left ventricular diastolic dysfunction in Nrf2 knock out mice is associated with cardiac hypertrophy, decreased expression of SERCA2a, and preserved endothelial function. *Free Radical Biology and Medicine* (Volume 89), pages 906-917

Zusammenfassung

Oxidativer Stress stellt einen zentralen Faktor für die Pathogenese kardiovaskulärer Erkrankungen dar. Er entsteht durch das Überwiegen oxidativer Radikale gegenüber antioxidativen Abwehrmechanismen in einer Zelle. Der Transkriptionsfaktor Nuclear-factor-erythroid-2-related-factor 2 (Nrf2) reguliert die Expression antioxidativer Enzyme. In Nrf2 Knockout (KO) Mäusen ist diese antioxidative Abwehr gestört und somit stellen sie ein wichtiges Modell zur Erforschung kardiovaskulärer Krankheiten dar. Hierbei blieb jedoch bisher unklar, ob der Knockout von Nrf2 die kardiale, koronare und peripher vaskuläre Funktion von Nrf2 KO Mäusen beeinflusst.

Diese Arbeit hypothetisiert, dass der Knockout von Nrf2 die kardiovaskuläre Funktion von Nrf2 KO Mäusen verändert. 6 Monate alte und 18 Monate alte Nrf2 KO Mäuse wurden mittels Echokardiographie, invasiver Blutdruck- und linksventrikulärer Druck-Volumen-Messung sowie anhand des Langendorff Modells analysiert und mit gleichaltrigen, genetisch unveränderten Wurfgeschwistern (Wildtyp Mäusen) verglichen. Die vaskuläre Funktion wurde als FMD von anderen Mitgliedern des Forschungsteams untersucht und wird ergänzend diskutiert.

Im Ergebnis zeigen junge und alte Nrf2 KO Mäuse im Vergleich zu Wildtyp Mäusen einen niedrigeren Blutdruck, eine diastolische Dysfunktion und reagieren weniger auf Inotropie und Lusitropie steigernde Medikamente (Arterenol, Ouabain, Isoproterenol). Die Herzen von Nrf2 KO Mäusen sind relativ zum Körpergewicht hypertrophiert, wohingegen die koronare Funktion von Nrf2 KO Mäusen erhalten ist. Diese Ergebnisse stehen im Einklang mit Experimenten, welche zeigen konnten, dass die periphere Gefäßfunktion von Nrf2 KO Mäusen erhalten ist und auf molekularer Ebene SERCA 2A weniger und eNOS vermehrt exprimiert werden. Es konnte somit eine Charakterisierung der kardialen Funktion sowie der koronaren und systemischen Gefäßfunktion erstellt werden.

Zusammenfassend wurde festgestellt, dass der Knockout von Nrf2 in Mäusen zu einer Verschlechterung der diastolischen Herzfunktion bei erhaltener Gefäßfunktion, was insgesamt zu einem niedrigeren Blutdruck von Nrf2 KO Mäusen führt.

Abstract

Oxidative stress, defined as an imbalance between oxidants and antioxidants, plays a central role in the pathogenesis of cardiovascular (CV) diseases. Among others the transcription factor Nuclear-factor-erythroid-2-related-factor 2 (Nrf2) controls the expression of antioxidant enzymes and contributes to the homeostasis of oxidant and antioxidant species. Knock out (KO) of Nrf2 leads to dysregulation of antioxidant defense. Therefore, genetically engineered Nrf2 KO mice were applied in different studies to evaluate the role of antioxidant defense. However, characterization of cardiac and coronary function of Nrf2 KO mice has not been undertaken so far.

This work is based on the hypothesis that dysregulation of redox state in Nrf2 KO mice may affect CV phenotype. Therefore, the CV function of young (6 months) and old (18 months) Nrf2 KO mice and their aged matched littermates were analyzed.

To characterize CV phenotype systemic hemodynamics, cardiac function, coronary function and vascular function were evaluated in these mice. Systemic hemodynamics was measured by Millar catheter. Cardiac function was assessed by echocardiography and in vitro in isolated hearts. Coronary function was assessed by flow and dilation of coronary arteries in isolated perfused hearts. Vascular function was assessed as FMD by other members of the research group and is discussed in context.

This work shows that young and old Nrf2 KO mice are hypotensive in comparison to same aged wildtype (WT) littermates. Cardiac function in Nrf2 KO mice is impaired, shown in diastolic dysfunction and lower response to inotropic medication. Accordingly, hearts of Nrf2 KO mice are hypertrophic as they show increased left ventricular mass to body weight ratio. Coronary function of Nrf2 KO mice is preserved. The results are consistent with other experiments showing myocardial downregulation of SERCA2a, preserved vascular function and upregulated eNOS in Nrf2 KO mice. Taken together impaired cardiac function and preserved vascular function result in lower blood pressure of Nrf2 KO mice.

Table of contents

Zusammenfassung.....	4
Abstract.....	5
Table of contents.....	6
List of figures	8
List of tables	9
1. Introduction	10
1.1. Regulation of systemic hemodynamics, cardiac and coronary function	10
1.2. Reactive oxygen species, oxidative stress and their effects in the cardiovascular system	15
1.3. The Keap1/Nrf2 redox system and oxidative defense.....	18
1.4. What is the role of Nrf2 in the cardiovascular system?.....	24
2. Hypothesis.....	26
3. Methods	27
3.1. Reagents and drugs	27
3.2. Animals.....	28
3.3. Echocardiographic assessment	29
3.4. Assessment of systemic hemodynamics in vivo (Millar-catheter)	31
3.5. Assessment of cardiac and coronary function ex vivo (isolated perfused heart)	36
3.6. Statistical analyses.....	40
4. Synopsis of pharmacological approach to study vascular and cardiac function.....	40
4.1 Adenosine	40
4.2 Bradykinin	43

4.3 2-ethyl-2-thiopseudourea.....	45
4.4 Isoproterenol and arterenol	46
4.5 Ouabain.....	47
5. Results.....	47
5.1. Systemic hemodynamics of Nrf2 KO mice	47
5.2. Cardiac function of Nrf2 KO mice	49
5.3. Coronary function of Nrf2 KO mice.....	60
6. Discussion.....	63
6.1. Nrf2 KO mice show lower blood pressure with unchanged heart rate	64
6.2. Left-ventricular function is dysregulated in Nrf2 KO mice.....	65
6.3. Coronary function is preserved in Nrf2 KO mice.....	69
6.4. Conclusion and outlook	71
List of abbreviations	74
References	78
Acknowledgement.....	86

List of figures

Figure 1: Systemic hemodynamics.....	11
Figure 2: Action potential of a ventricular myocyte.....	11
Figure 3: Cardiac excitation-contraction coupling.....	12
Figure 4: cVSMC -coronary vascular smooth muscle cell- contraction	14
Figure 5: Reduction of O ₂ to H ₂ O	15
Figure 6: NO signaling in the vasculature.....	17
Figure 7: Oxidative stress.....	18
Figure 8: Physiological degradation of Nrf2	19
Figure 9: Activation of Nrf2 by increased levels of ROS	20
Figure 10: Oxidative defense	21
Figure 11: Target genes of Nrf2	23
Figure 12: Outline.....	26
Figure 13: Mitral valve Doppler profile	30
Figure 14: Surgical steps for insertion of Millar catheter	32
Figure 15: Blood pressure curve	33
Figure 16: Pressure volume loop	33
Figure 17: Apparatus Isolated Heart	37
Figure 18: Langendorff experimental procedure	39
Figure 19: Adenosine receptors.....	41
Figure 20: Endothelium dependent vasodilation of adenosine.....	42
Figure 21: H ₂ O ₂ mediated adenosine response	43
Figure 22: Vascular bradykinin response	44
Figure 23: NO mediated vasorelaxation.....	45
Figure 24: Blood pressure of young and old Nrf2 KO and WT mice.....	48
Figure 25: Diastolic function of young Nrf2 KO mice	51
Figure 26: LV-contractility baseline and after Arterenol treatment	53
Figure 27: LV- contractility baseline and after ouabain treatment.....	54
Figure 28: Contractility of isolated hearts of 6 months old mice.....	55
Figure 29: Cardiac function of young and old WT mice.....	56
Figure 30 Cardiac function of young and old Nrf2 KO mice.....	57

Figure 31: Contractility of 18 months old Nrf2 KO and WT mice.....	58
Figure 32: Contractility of old hearts after stimulation with Iso.....	59
Figure 33: Coronary flow baseline and after drug treatment.....	60
Figure 34: Coronary flow of young and old mice	61
Figure 35: Coronary flow of young and old mice	62
Figure 36: Outline.....	63

List of tables

Table 1: Parameters obtained in b-mode parasternal long axis view.....	30
Table 2: Mitral valve Doppler parameters measured in four-chamber view .	31
Table 3: Group design for Millar assessment.....	34
Table 4: Parameters of blood pressure assessment.....	35
Table 5: Parameters of in vivo left ventricular pressure volume assessment	35
Table 6: Parameters obtained ex vivo in isolated hearts.....	38
Table 7 exclusion criteria for isolated perfused hearts	39
Table 8: Blood pressure of young Nrf2 KO mice	48
Table 9: Blood pressure after administration of ETU	49
Table 10: Echocardiographic assessment of Nrf2 KO mice.....	50
Table 11: LV-pressure-volume relationship in Nrf2 KO mice.....	52
Table 12: LV- pressure-volume relationship after Arterenol administration .	52
Table 13: Baseline coronary flow.....	60

1. Introduction

Cardiovascular diseases represent the major cause of death in the industrialized nations. In Germany treatment of patients with manifest cardiovascular diseases incurs costs of 36 billion € [2], which is 15 % of total healthcare spending [2]. Years of research have explored the pathogenesis of these diseases and provided novel therapeutic concepts, which have contributed to decrease mortality from cardiovascular diseases in the last years [3]. However, there are still unanswered questions in the molecular mechanisms of cardiovascular diseases.

Since Sies et al. introduced the concept of oxidative stress 30 years ago [4], evidence has been provided that dysregulation of the oxidant/antioxidant homeostasis plays a major role in the development of cardiovascular diseases such as atherosclerosis [5-7], hypertension [8, 9] and heart failure [10, 11].

1.1. Regulation of systemic hemodynamics, cardiac and coronary function

To ensure sufficient circulation, the cardiovascular system is dependent on adequate blood pressure. The mean arterial pressure (MAP) is dependent on cardiac output (CO) and systemic vascular resistance (SVR) according to the equation: $MAP = CO \times SVR$ [12]. These three parameters are the components of hemodynamic homeostasis (Figure 1). CO is determined by stroke volume and heart rate [12]. Stroke volume is dependent on the size of the ventricle, preload, afterload and the contractility of the heart [12]. Contractility is the power and velocity with which the cardiac muscle contracts [12]. Peripheral resistance is influenced by physical factors like characteristics of the blood flow itself, viscosity of blood, distending pressure and diameter of the vessels according to the Poiseuille equation [12]. The main target of the numerous dynamic control systems is the vessels diameter resulting from a homeostasis of vasoconstriction and vasorelaxation. This homeostasis is regulated by humoral vasoactives, the autonomic nerve system (ANS) and local autoregulation [12, 13].

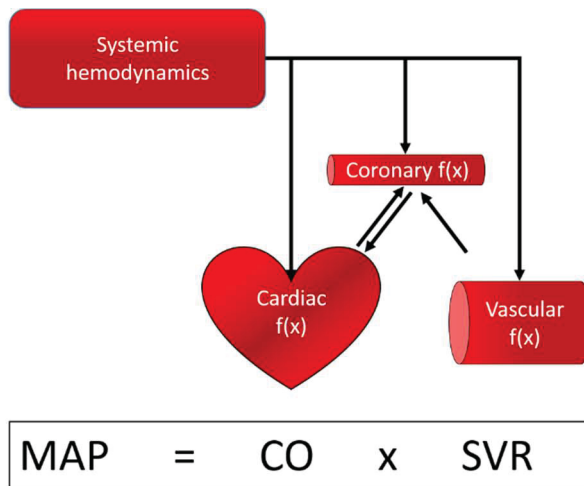


Figure 1: Systemic hemodynamics
 Systemic hemodynamics present the homeostasis between cardiac and vascular function. The coronary arteries serve a special role of the vasculature because of their paracrine interaction with the cardiac myocytes itself. Mean arterial pressure (MAP) is dependent of cardiac output (CO) and systemic vascular resistance (SVR).

Contraction of cardiac cells starts with the action potential which is followed by several intracellular mechanisms enabling the excitation-contraction coupling [14]. The action potential of ventricular myocytes can be divided into 5 sections (Figure 2) [14].

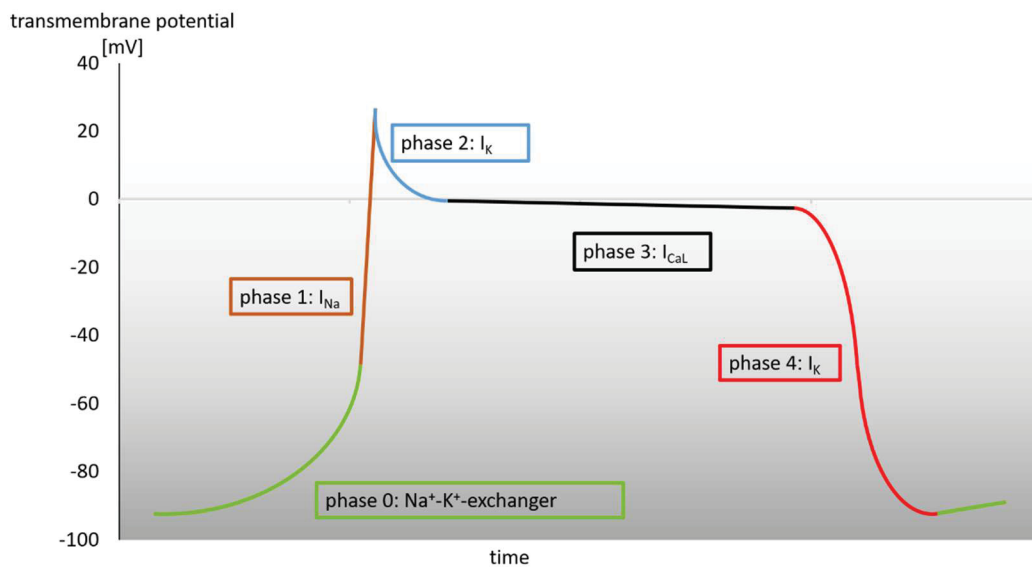


Figure 2: Action potential of a ventricular myocyte
 Different phases of ventricular action potential and the predominant currents.

The resting potential is about -96 mV and is stabilized by Na⁺-K⁺-exchanger [14]. When the cell gets stimulated and the membrane potential is elevated over the threshold of -40 mV, fast Na⁺-channels open and generate an inward Na⁺-current (I_{Na}) which depolarizes the cell until it reaches a peak at about +30 mV [14]. A transient K⁺-outward current (I_k) decreases the potential before L-

type Ca^{2+} -channels (Figure 3) open which generate an inward Ca^{2+} -current (I_{CaL}). The I_{CaL} enables the plateau phase. The plateau phase voltage is about 0 mV and extends the duration of cardiac action potential up to 300 ms. The final repolarization is characterized by an outward K^+ -current (I_{K}) [14]. The important step for excitation-contraction coupling (Figure 3) is the I_{CaL} . The influx of Ca^{2+} triggers ryanodine receptors (RyR) at the sarcoplasmic reticulum to open [14]. That results in a massive Ca^{2+} release from the sarcoplasm into cytoplasm, so called calcium sparks [15, 16]. These Ca^{2+} sparks elevate the intracellular Ca^{2+} concentration from 10^{-7} mmol/l to 10^{-5} mmol/l. Ca^{2+} diffuses through the cell and binds to troponin C resulting in a conformation change of the myofilaments and enabling the muscle contraction [14].

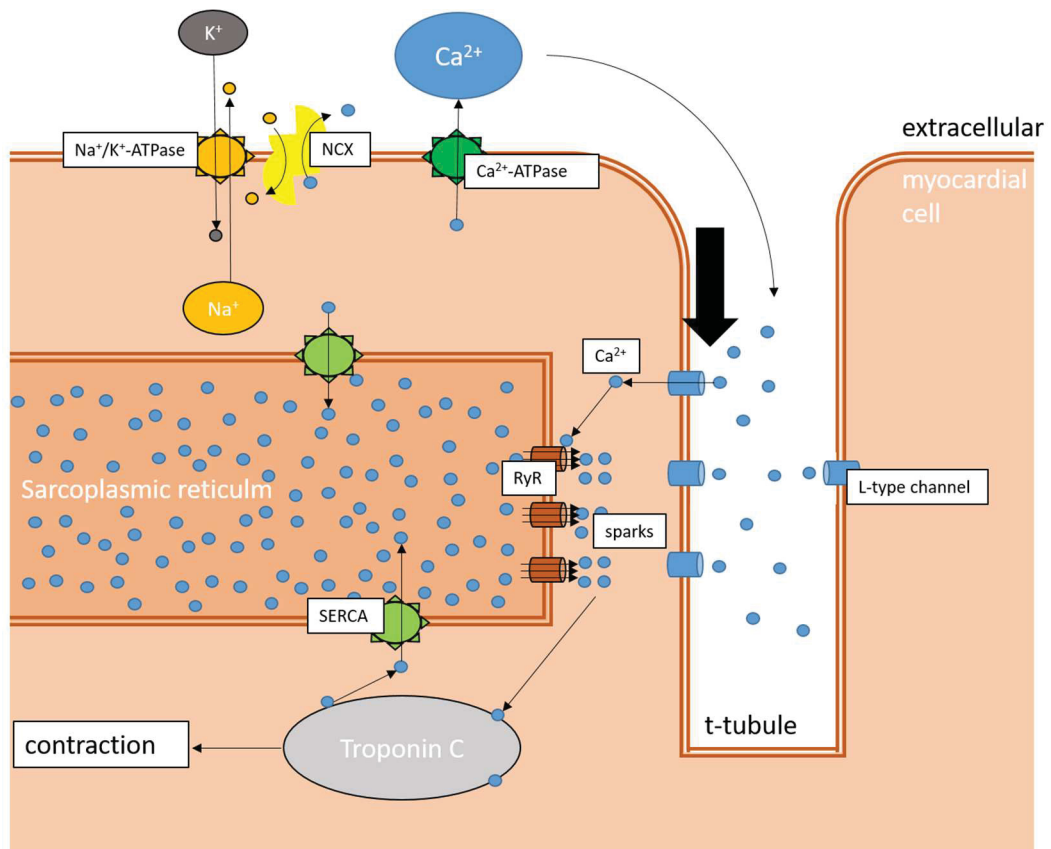


Figure 3: Cardiac excitation-contraction coupling

Depolarisation (black arrow) opens L-type Ca^{2+} channels in the membrane of the t-tubule. Ca^{2+} influx triggers ryanodine receptors (RyR) to release Ca^{2+} sparks which bind to Troponin C and activate the contractile apparatus. Ca^{2+} is removed into the sarcoplasmic reticulum by sarcoplasmic/endoplasmic reticulum Ca^{2+} ATPase (SERCA). Ca^{2+} -ATPase and $\text{Na}^+/\text{Ca}^{2+}$ -antiporter (NCX) transport Ca^{2+} out of the cell.

Decreasing cytoplasmic Ca^{2+} concentration will end the contraction by ceasing to bind to troponin C. Ca^{2+} gets actively pumped back into sarcoplasmic reticulum by Sarcoplasmic/endoplasmic reticulum calcium ATPase (SERCA). Additional Na^+ - Ca^{2+} -exchanger (NCX) removes intracellular Ca^{2+} (Figure 3) [14].

Coronary circulation is needed to supply the myocardium with oxygen and nutrients. In resting conditions the oxygen extraction of the coronary arteries is already about 70 %. During exercise myocardial oxygen consumption can increase as much as fivefold which can only occur by a similar augmentation of coronary blood flow [17]. The coronary blood flow is only possible while diastole, which is limited by heart rate. Sufficient increase of flow is therefore highly dependent on decrease of coronary resistance to meet the increased oxygen demand.

Following the branching of vessels, the coronary circulation can be divided into 3 compartments [18]. The big epicardial vessels build the first compartment and offer only little resistance to coronary flow. The second compartment is made up of small coronary arteries which are known as resistance microvessels because they provide about 60 % of total coronary resistance. The small intramyocardial capillaries make up the third compartment and provide 25 % of resistance. The last 15 % resistance is provided by the venular compartment. While exercising or ischemia the vessels of the second and third compartment are able to dilate and decrease the coronary resistance by 70 % [18]. This decrease in resistance is followed by an increase in coronary blood flow which is called hyperemic response. The margin between maximum hyperemic coronary flow and the basal coronary flow is called coronary flow reserve. In experimental settings and recently in clinical trials coronary flow reserve is used to evaluate the coronary function and predict the risk for hard cardiovascular events [19-22]. It has been shown that decrease of coronary flow reserve is a critical step in the development of hypertension, left ventricular hypertrophy, atherosclerosis and infarction [19-24]. The possibility of hyperemic response is therefore a major characteristic of a healthy cardiovascular system.

Coronary dilation occurs due to the relaxation of coronary vascular smooth muscle cells (cVSMC). Relaxation of coronary vascular smooth muscle cells is mediated by mechanical autoregulation (rise in blood pressure), local metabolites (such as CO_2 , H^+ , K^+ , adenosine), endothelium derived substances (NO, prostaglandin I_2 (PGI_2), H_2O_2), hormones (catecholamines, Angiotensin II), ANS (sympathetic and parasympathic stimulation). The final common pathway of all relaxing and contracting mediators is the interplay of myosin-light-chain-kinase (MLCK) and myosin-light-chain-phosphatase (MLCP) (Figure 4) [14].

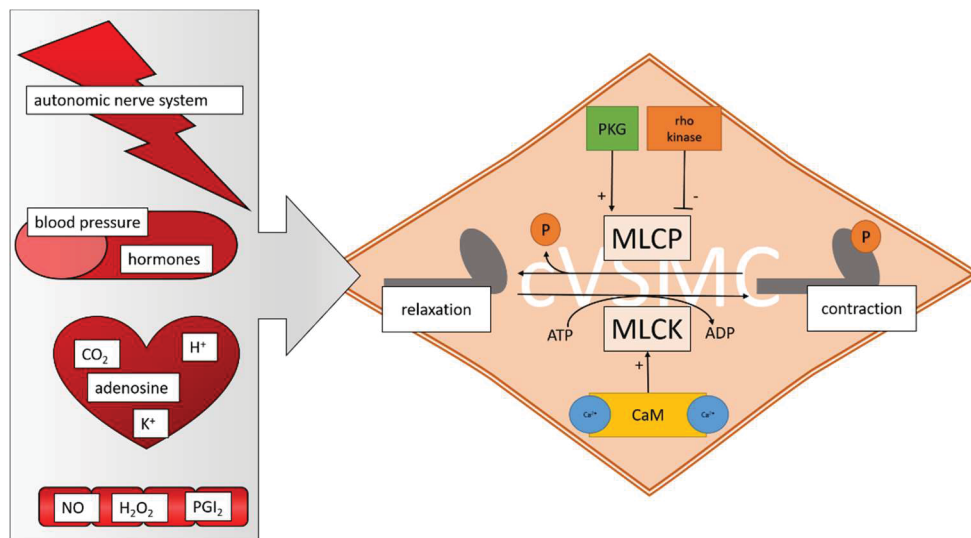


Figure 4: cVSMC -coronary vascular smooth muscle cell- contraction

Phosphorylation of myosin enables contraction of smooth muscle cells. Dephosphorylation relaxes smooth muscle cells. Myosin light chain phosphatase (MLCP) is regulated by protein kinase G (PKG) and rho kinase. Myosin light chain kinase (MLCK) is activated by Ca^{2+} -Calmodulin-complex (CaM). Contraction and relaxation of coronary vascular smooth muscle cells (cVSMC) are mediated by the autonomic nerve system, mechanical autoregulation (blood pressure), hormones, local metabolites from the myocardial cells, and endothelium-derived substances (NO, H_2O_2 , PGI_2). Only selected mediators known are shown.

Increased Ca^{2+} levels activate calmodulin, which activates MLCK. Subsequently, MLCK phosphorylates and activates the myosin filament resulting in contraction. MLCP dephosphorylates myosin and relaxes the smooth muscle cell. MLCP is also activated by phosphorylation, for example by protein kinase G (PKG).

1.2. Reactive oxygen species, oxidative stress and their effects in the cardiovascular system

Reactive oxygen species (ROS) play a central role in the development of cardiovascular disease [11]. High concentrations of reactive oxygen species lead to oxidative stress. Oxidative stress causes oxidative damage which is an important keystone in the development of cardiovascular diseases.

Reactive oxygen species (ROS) are generated when molecular oxygen (O_2) is reduced to water (Figure 5). The intermediate products have vast amounts of free energy and are very reactive, thus they react with their surrounding molecules and thereby change the structure of DNA, RNA, proteins and lipids [11, 25-31].

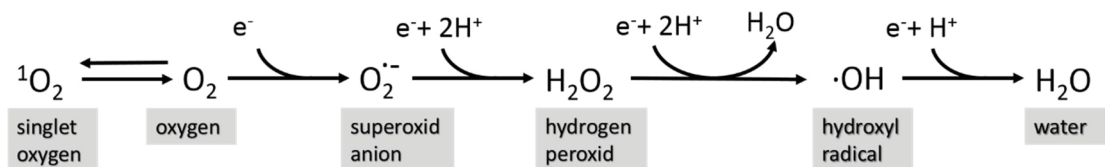


Figure 5: Reduction of O_2 to H_2O

O_2 gets reduced to H_2O in numerous enzymatic reactions. Intermediate products are able to leak as free radicals. Figure adapted from Posselt, 2006 [32].

O_2 is reduced to superoxide ($O_2^{\cdot-}$) as a side-product in various enzymatic reactions, for example at complex I and III of electron transfer chain in the mitochondria [33-35]. Superoxide dismutase (SOD) forms hydrogen peroxide (H_2O_2) and O_2 by disproportionation of 2 superoxides [32, 33]. H_2O_2 does not contain an unpaired electron and is therefore not regarded as a free radical [32]. However, in the presence of Fe^{2+} or other transition metals H_2O_2 can be converted to hydroxyl radical ($\cdot OH$) (Fenton-/Haber-Weiss- reaction) which is a very aggressive oxidant [32]. $\cdot OH$ has a half-life of less than 1 ns. Reactions of $\cdot OH$ with its surrounding compounds generate further radicals like alkyl radicals ($R-\dot{C}H$) and peroxy radicals ($ROO\cdot$) [32].

Beside mitochondrial enzymes, there are other enzymes which create ROS. One example is the family of cytochrome P450 oxidases (CYPs) which is involved in the metabolism of endo- and xenobiotics. CYPs also enhance the generation of ROS and thereby contribute to ischemic-reperfusion heart

injuries [36]. Other enzymatic sources of ROS are lipoxygenases, xanthine oxidases, cyclooxygenases and NADPH oxidases. ROS are also present as pollutants from the atmosphere and are generated during irradiation by UV-light, x-rays or gamma-rays [25].

Although ROS are often held responsible for lethal cellular damage, ROS fulfill essential functions. In peroxisomes for example, they are used to break down long fatty acids (beta-oxidation) [33]. Furthermore, the destructive effect of ROS is used by granulocytes and macrophages to defend the body from infections (oxidative burst) [33]. The use of ROS as messenger molecules is called redox signaling [37]. Because being more stable H_2O_2 has the ability to diffuse through membranes [38] and takes an important role in redox signaling. Generated from endothelial cells, H_2O_2 diffuses to smooth muscle cells and causes relaxation [39].

Besides ROS, reactive nitrogen species (RNS) also play a role in redox signaling [25, 40]. Nitric oxide (NO) generated by NO synthase (NOS) serves as a physiological signaling molecule [40-42]. NOS catalyzes the oxidation from L-arginin to L-citrullin, consuming NADPH and O_2 and producing $NADP^+$, H_2O and NO [40]. Different isoforms of NOS are known. Endothelial NOS (eNOS) is expressed in endothelial cells. NO diffuses to smooth muscles cells and causes vasodilation [43-46] (Figure 6). Furthermore, eNOS is a central player in endothelial homeostasis coupling the blood flow to long-term vascular remodeling, thus eNOS and generated NO have long-term impact on vascular health and disease [47].

Similar to ROS, physiological NO signaling is characterized by a delicate homeostasis between beneficial function and harmful modifications. NO and superoxide together form peroxynitrite and other strong oxidants [25]. All radicals generated from NO and O_2^- are called reactive nitrogen species (RNS) and overproduction of RNS is called nitrosative stress [25]. In the interest of simplicity, the terms “ROS” and “oxidative stress” also include “RNS” and “nitrosative stress” for the following thesis, unless explicitly excluded.

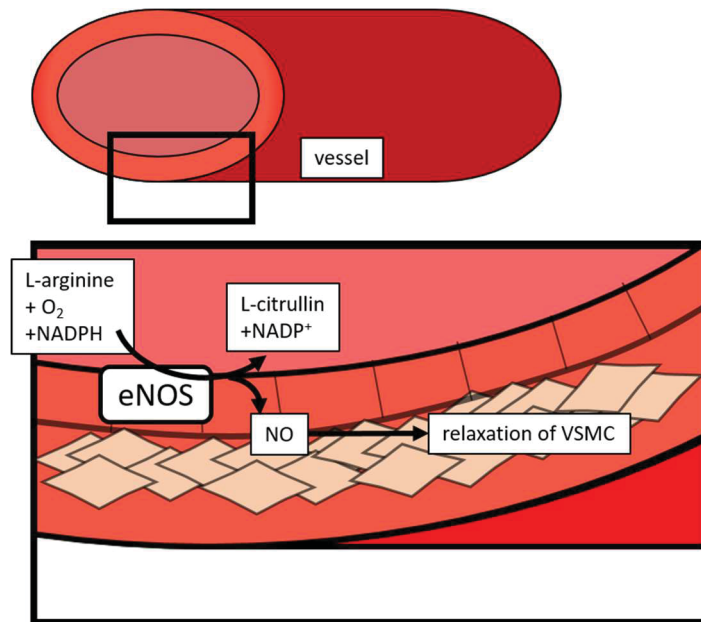


Figure 6: NO signaling in the vasculature

NO is built by endothelial cells and diffuse into VSMC to cause vasorelaxation.

Every aerobe living cell has a susceptible pro-oxidant-antioxidant balance which is essential for its physiological function [4]. A shift towards oxidizing agents is called oxidative stress and numerous studies have shown that oxidative stress impairs normal cellular function, causes inflammation, diseases and death [37] (Figure 7). Therefore, the healthy cell has developed enzymes to detoxify reactive species and defend the cell from oxidative stress [48].

Harman first introduced the theory of aging being processed by free radicals in 1956 [49]. Since then evidence has been published, which confirms that aging and age-related diseases are associated with accumulation of oxidative damaged proteins [27-29, 37, 50-52]. This oxidative damage is characterized by the formation of different kinds of intra- and inter-protein cross linkages [25]. For example cysteine residues are susceptible to ROS and oxidation of the sulfhydryl group forms S-S-crosslinks. However, these oxidations are reversible and the cross links can be repaired by thiol transferases [25]. This is one mechanism of redox signaling, because the generated disulfide bonds are able to change the conformation of proteins, which may result in activation or inactivation of enzymes.

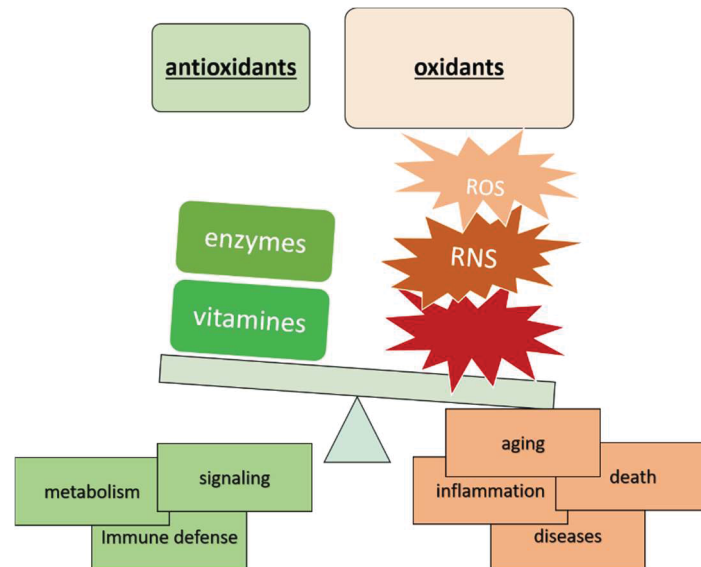


Figure 7: Oxidative stress

Oxidative stress is the imbalance between oxidants and anti-oxidants, leading to a disruption of redox signaling and/or molecular damage. Reactive oxygen species (ROS) and reactive nitrogen species (RNS) are physiological produced for cell signaling. Ischemia, inflammation, radiation and metabolism of xenobiotics can cause an increase of oxidants, which have detrimental effects on DNA, RNA, proteins, lipids and lead to dysregulation of various cellular pathways, resulting in miscellaneous pathologies.

When ROS react with lipids, proteins, DNA and RNA they are able to cause structural damage [25, 31]. Cells are able to repair these damages to a certain extent, but dependent on the damaged structure and magnitude of injury ROS may lead to apoptosis, necrosis and inflammation [25, 30, 48] which results in atherosclerosis, heart infarction and stroke [6, 7, 53-55]. Increase of ROS has also been linked to age-dependent decrease of cardiac function and heart failure [26, 56, 57].

1.3. The Keap1/Nrf2 redox system and oxidative defense

Aerobe living cells have developed an elaborated system of repair and defense mechanisms to counter oxidative stress. Repair enzymes are able to recover the oxidative damages.

Besides this, there is also an abundance of mechanisms immediate directed against ROS. This oxidative defense detoxifies ROS and keeps the homeostasis

of physiological ROS generation without oxidative stress [48]. Therefore, antioxidant enzymes are upregulated if the concentration of ROS is increasing inside a cell. The expression of antioxidant enzymes is regulated by transcription factors sensing the amount of ROS and regulating the transcription of the antioxidant enzymes.

The antioxidant response element (ARE) is a binding sequence in the DNA upstream of genes of many antioxidant enzymes [58]. One of the transcription factors which activate ARE is the nuclear-factor-erythroid-2-related-factor 2 (Nrf2). Nrf2 was first recognized in the early 1990's as a member of the nuclear factor erythroid 2 (NF-E2) family which plays a major role in erythropoiesis [59]. Later, it was discovered that Nrf2 mediates ARE-induced transcription of antioxidant enzymes and phase II detoxification enzymes [60-63].

Nrf2 is ubiquitously expressed in every tissue of mammals. In physiological "unstressed" conditions Nrf2 protein has a short half-life of about 20 minutes. Kelch like ECH-associated protein 1 (Keap1) binds to Nrf2 and helps Cullin 3 (Cul3) to ubiquitinate Nrf2. After ubiquitination Nrf2 is degraded by proteasomes (Figure 8) [64].

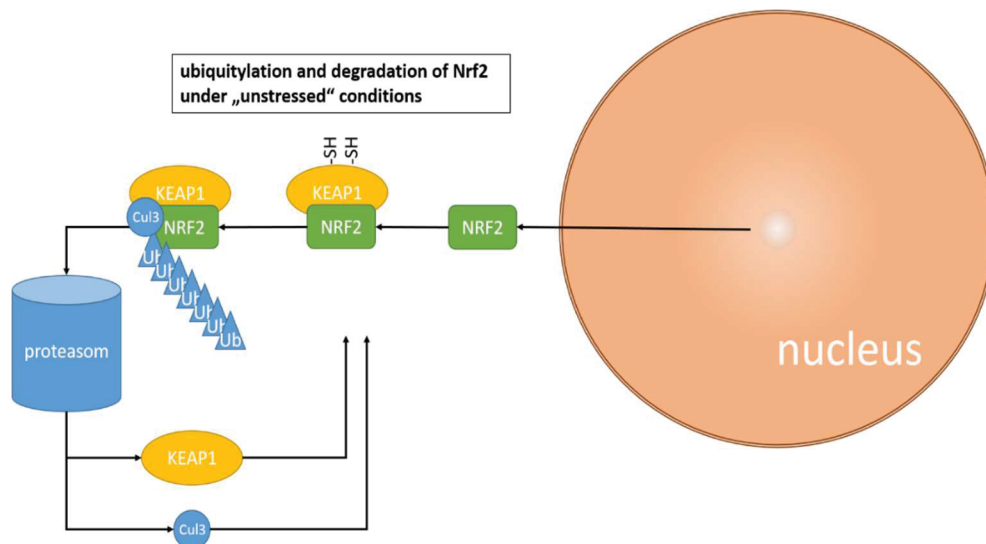


Figure 8: Physiological degradation of Nrf2

Physiological ubiquitination and proteasomic degradation of Nrf2 while low concentration of reactive oxygen species. Kelch like ECH-associated protein 1 (Keap1) binds to Nrf2 and helps Cullin 3 (Cul3) to ubiquitinate (Ub) Nrf2. After ubiquitination Nrf2 is degraded by proteasomes. Keap1 and Cul3 are not degraded and free to ubiquitinate other Nrf2.

Increasing levels of ROS are able to interrupt the binding of Keap1 thus ubiquitination and degradation of Nrf2 is abrogated and Nrf2 can translocate into the nucleus. There, Nrf2 forms a heterodimer with small MAF kinases and enhances the transcription of target genes. There are two ways known of how this interruption of Nrf2 degradation is arranged (Figure 9) [59, 64, 65].

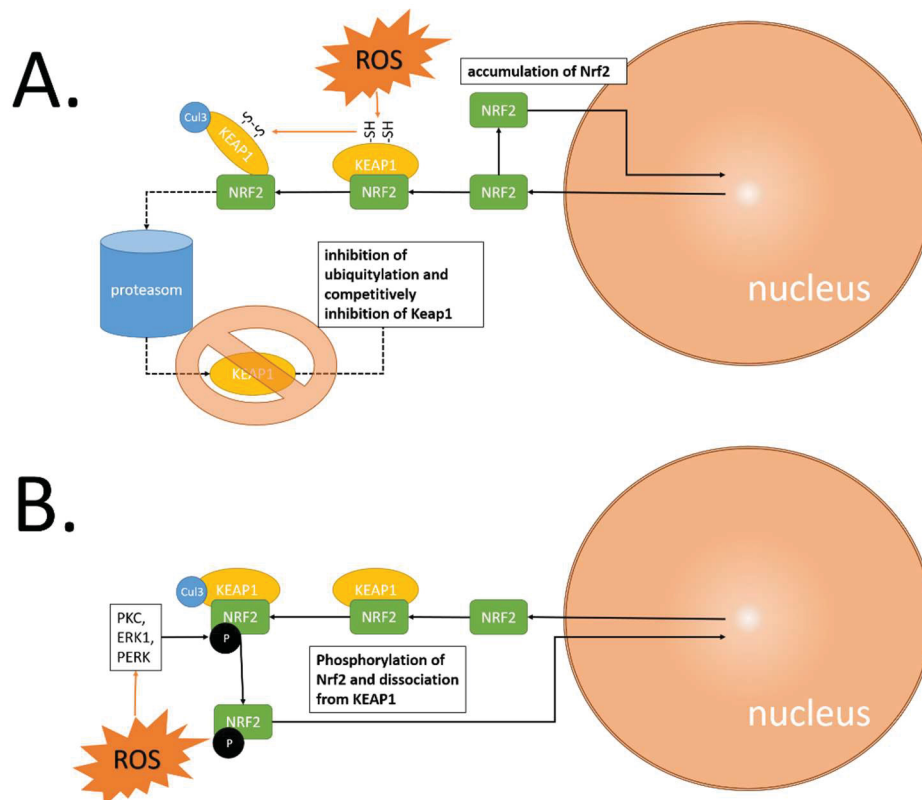


Figure 9: Activation of Nrf2 by increased levels of ROS

A. Free radicals oxidize Keap1 which changes conformation and disables further ubiquitylation of Nrf2 without dissociating from Nrf2. Degradation of Nrf2 is uncoupled while Keap1 is competitively inhibited and subsequent transcribed Nrf2 accumulates and is free to translocate into the nucleus.

B. Phosphorylation of Nrf2 leads to dissociation from Keap1 and Nrf2 is free to translocate.

Keap1 contains cysteine residues which can be oxidized by ROS to generate disulfide bonds within Keap1 protein. Disulfide bond formation changes conformation of Keap1 thus Cul3 can no longer ubiquitinate Nrf2. As a result, Nrf2 is not degraded and competitively inhibits Keap1. This will accumulate Nrf2 in cytosol and support translocation into the nucleus. It has also been shown that Nrf2 can be phosphorylated by several kinases such as PKC, ERK1

or PERK. Phosphorylation leads to dissociation of Nrf2 from Keap1 thus Nrf2 is free to translocate into the nucleus [59, 64, 65].

Nrf2 contains a basic leucine zipper domain (bZIP) which is typical for eukaryotic transcription factors [48, 58, 59, 64-66]. The bZIP is formed by an alpha-helix with a lot of basic aminoacids like lysin or arginine. Every 7th amino acid is hydrophobic, usually leucine. This hydrophobic character allows dimerization of proteins with bZIP. The two alpha helices form a coiled-coil which can easily attach to the DNA-double-helix and the positive loaded arginine or lysin are able to bind the negative loaded DNA-backbone. Besides Nrf2, there are also Maf-, c-Jun- and c-Fos-proteins with bZIP. After nuclear translocation Nrf2 forms heterodimer with those bZIP containing transcription factors and bind to the ARE region on the DNA [48, 58, 59, 64-66]. Binding to ARE promotes the transcription of the upstream encoded genes.

Increase of ROS activates Nrf2 which increases oxidative defense. The antioxidant enzymes detoxify ROS. As a first step superoxide anion is converted to H₂O₂ by SOD (Figure 10). H₂O₂ is the target for different antioxidant enzymes such as catalase or glutathione-peroxidase (GPx). If production of H₂O₂ is higher than its elimination and in the presence of “free” transition metals (e.g. Fe²⁺), H₂O₂ is converted to hydroxyl radical (\cdot OH) [32].

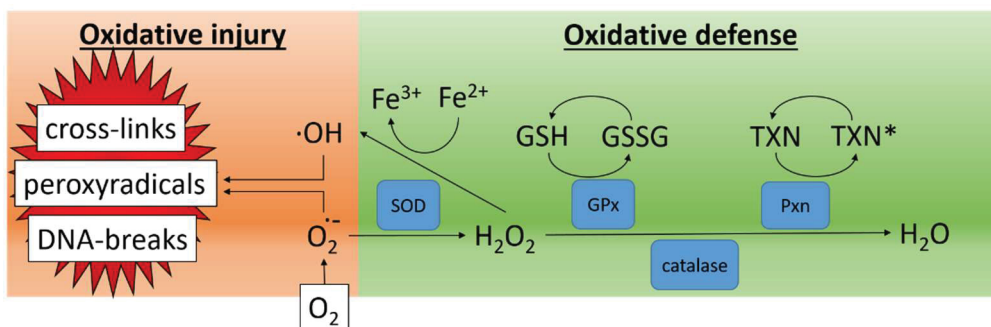


Figure 10: Oxidative defense

Superoxide radical is detoxified by Superoxide Dismutase (SOD). Three main mechanisms detoxify generated H₂O₂, which otherwise would be reduced to hydroxyl radical (\cdot OH) by Fenton reaction. Superoxide and hydroxyl radical oxidize other molecules causing oxidative injury. GPx (glutathione-peroxidase); Glutathione (GSH=reduced, GSSG=oxidized); Pxn (peroxiredoxin); Thioredoxin (TXN=reduced, TXN*=oxidized)

Beginning from hydroxyl radical there are various kinds of radicals. These radicals are eliminated by different antioxidant enzymes. This large family of antioxidant enzymes is dependent on cofactors which work as reducing agents. The most abundant endogenous antioxidant cofactors are glutathione (GSH) and nicotinamide-adenine-dinucleotide-phosphate (NADPH) [48, 67]. The synthesis, utilization and regeneration of GSH and NADPH are regulated by Nrf2 (Figure 11).

GSH is a tripeptide formed of glutamate, cysteine and glycine [33]. The thiol-group of the cysteine residue serves as an electron donor and enables other enzymes to detoxify ROS. The ligation of glutamate with cysteine is the rate-limiting step in GSH synthesis. Nrf2 enhances both the expression of glutamate-cysteine-ligase (GCL) and the concentration of cysteine by increasing the transcription of the cysteine/glutamate transporter (XCT) [48]. XCT enhances intracellular cysteine concentration. Cysteine is reduced to cysteine by GSH or by thioredoxin reductase (TXNRD) which is also up-regulated by Nrf2 [48] (Figure 11).

GSH is a cofactor of diverse ROS-detoxifying enzymes such as glutathione peroxidase (GPx) and several glutathione S-transferases (GSTA), which are also regulated by Nrf2 [48]. As a cofactor GSH is converted to its oxidized form and linked to another oxidized GSH [33]. The resulting hexapeptide is called glutathione disulfide (GSSG). GSH is regenerated from GSSG by Nrf2-induced glutathione reductase (GSR). GSR utilizes NADPH to break down the disulfide bond. The generated NADP^+ is recovered in the pentose-phosphate-pathway [33], which is also influenced by Nrf2 (Figure 11).

NADPH is also needed to regenerate thioredoxin (TXN). TXN is a group of antioxidant molecules, which include a cysteine. Similar to GSH, the thiol-group serves as an electron donor as it forms disulfide bonds with another cysteine at the active site of TXN [33]. TXN is used to reduce peroxiredoxin (PXN) which is an antioxidant that catalyzes the reduction of hydroperoxides (ROOH). Nrf2 is also increasing the transcription of PXN and TXN [48] (Figure 11).

Besides increasing the transcription of ROS-detoxifying enzymes, Nrf2 has a direct impact on ROS generation as it controls important enzymes of intracellular iron homeostasis. Free iron is essential for generating hydroxyl radical (Fenton-reaction). Nrf2 controls hem oxygenase 1 (HO1), ferritin light chains and ferritin heavy chains. In fact, Nrf2 activation leads to Fe²⁺ sequestration from hem containing enzymes to intracellular Fe²⁺ stores [48] (Figure 11).

In brief, target-genes of Nrf2 control the usage production and regeneration of GSH, NADPH and TXN, as well as iron sequestration (Figure 11). Therefore, activation of Nrf2 enhances the full extent of enzymatic cellular oxidative defense. Knockout of Nrf2 on the opposite is followed by dysregulation of antioxidant defense systems [1, 64].

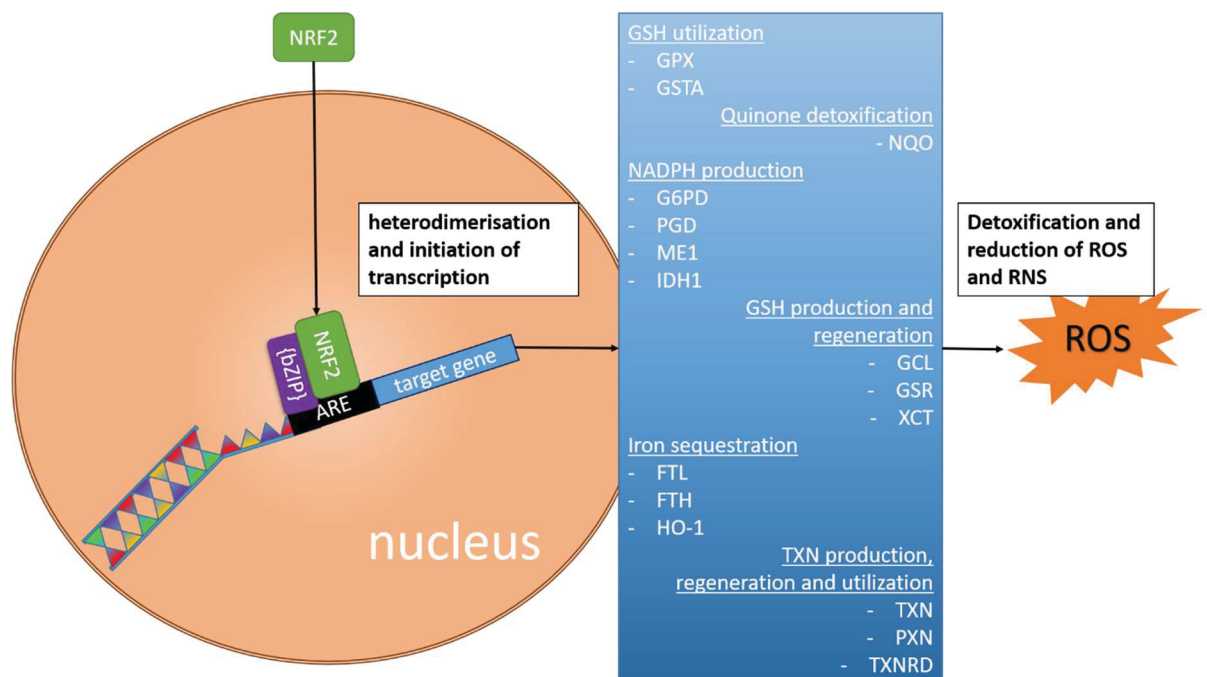


Figure 11: Target genes of Nrf2

Nrf2 heterodimerizes with other bZIP containing proteins and bind to the antioxidant response element (ARE) promoting the transcription of several genes: Glutathione S-transferase (GSTA); Glutathione peroxidase (GPX); glutamate–cysteine ligase (GCL); cysteine/glutamate transporter (XCT); glutathione reductase (GSR); NAD(P)H:quinone oxidoreductase (NQO); Ferritin light chain (FTL); Ferritin heavy chain (FTH); haem oxygenase 1 (HO-1); glucose-6-phosphate dehydrogenase (G6PD), phosphoglycerate dehydrogenase (PHGDH), malic enzyme 1 (ME1); isocitrate dehydrogenase 1 (IDH1); thioredoxin (TXN); thioredoxin reductase (TXNRD), peroxiredoxin (PXN)

Adapted from Gorrini et al. [48] and modified.

1.4. What is the role of Nrf2 in the cardiovascular system?

Genetically engineered Nrf2 knock-out (Nrf2 KO) mice show dysregulated oxidative defense mechanisms and could be considered as a model of chronic adaptation of the organism to oxidative stress. Nrf2 KO mice have been used in research and their use has contributed to a deeper understanding of the role of oxidative stress in fracture healing [68], carcinogenesis [69], diabetes mellitus [70], neurodegeneration [71] and cardiovascular diseases [1, 53, 72-74].

With focus on cardiovascular diseases it has been shown that Nrf2 KO mice are more susceptible to cardiac remodeling which is the myocardial answer to cardiac injury or pressure/volume overload. After pharmacological induction of hypertension as well as after surgical constriction of the aorta, hearts of Nrf2 KO mice become more hypertrophic than wild-type hearts [72, 73]. Angiogenesis after infarction is also declined by Nrf2 knock-out [75].

There is also evidence that Nrf2 plays a role in atherosclerosis, because HO-1 is known to protect against inflammation in vascular tissue [76], which is generally accepted as a key step in the development of atherosclerosis. Furthermore, atherosclerosis is characterized by endothelial foam cell formation and induction of adhesion molecules on the surface of endothelial cells. Activation of Nrf2 is able to protect endothelial cells of this induction [77] and deficiency of Nrf2 is linked to augmented foam cell formation and atherosclerosis [78]. In contrast, Nrf2 deficiency has a protective effect towards atherosclerosis when it is connected with ApoE deficiency, a genetically engineered model of hypercholesterolemia [53, 74].

Dysregulation of Nrf2 is important in the pathogenesis of diabetes mellitus and diabetic vascular disease [79, 80]. Additionally, it has recently been shown that Nrf2 KO aggravates chronic hypoxia-induced cardiopulmonary alteration, whereas Keap1 deficiency has a protective effect [81]. Nrf2 KO mice have been used to get further understanding of the cardioprotective effects of drugs and nutritional supplements [82]. There has been growing interest in targeting the Nrf2/Keap1 pathway for future pharmacological therapies [55] of cardiac and vascular diseases.

Furthermore, Nrf2 KO mice might be used as a model for cardiovascular aging. Several investigations have shown that most of the ARE-promoted antioxidative enzymes decrease with aging and that Nrf2 activity declines with increasing age [50]. This might be a reason for higher cardiovascular risk at advanced age. As a result, aging is accompanied by decline in GSH levels [83]. Accordingly, dysregulation of oxidative defense has been shown to reduce the life span of worms [84] and increase of oxidative defense by overexpression of cardiac catalase prolongs life span of mice [85]. However, there are also few studies showing no change or increase in antioxidant capacity [50] varying from the studied organism (mice, rat, primate, human) and organ. For the cardiovascular system, all published studies have so far shown that Nrf2 and dependent protein expression deteriorate with increased age [50].

It is conceivable that cardiovascular impairment of Nrf2 KO mice worsens with increased age because other impacts of Nrf2 deficiency are also age dependent. Age dependent hearing loss for example occurs prematurely in Nrf2 KO mice, even with no differences in hearing at the age of 3 months [86].

In short, Nrf2 has gained much attention in cardiovascular research and it is assumed that Nrf2 has an important role in cardiovascular function, but a profound understanding is missing. Nrf2 KO mice may represent a useful model of cardiac remodeling, cardiovascular aging and atherosclerosis. However, there are no studies comparing the basal cardiovascular functions of Nrf2 KO mice with WT littermates. Furthermore, cardiovascular assessment of aged Nrf2 KO mice is also missing.

2. Hypothesis

This work is based on the hypothesis that dysregulation of redox state in Nrf2 KO mice may affect cardiovascular phenotype (Figure 12).

The aim of this thesis is to characterize the cardiovascular function of young and old Nrf2 KO mice. Systemic hemodynamics, cardiac function and coronary function of young (6 months) and old (18 months) Nrf2 KO and WT mice are analyzed to investigate whether cardiovascular phenotype of Nrf2 KO mice is altered.

Systemic hemodynamics, cardiac function and vascular function are assessed *in vivo*. Cardiac function and coronary function are assessed *ex vivo* in isolated hearts of mice.

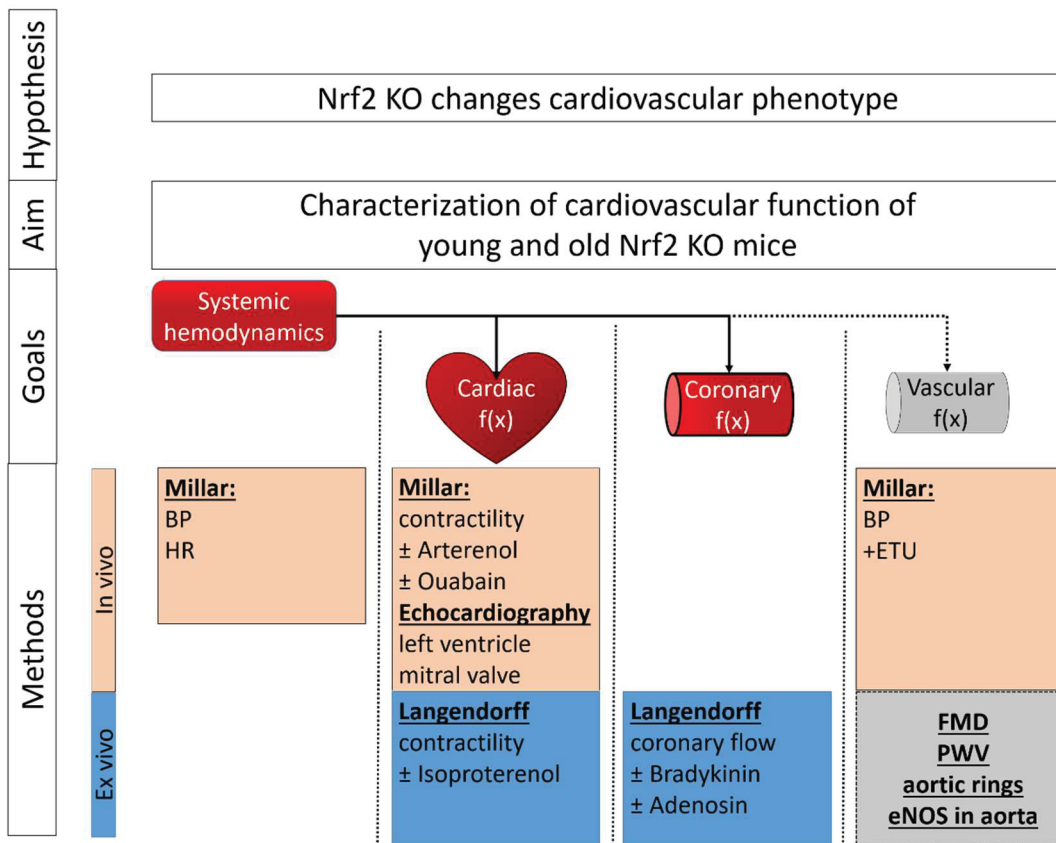


Figure 12: Outline

The thesis follows the question whether the absence of Nrf2 affects hemodynamics, cardiac function and coronary function of mice. Peripheral vascular function was assessed by others (grey) and is discussed in context. f(x) function; BP blood pressure; HR heart rate;

3. Methods

3.1. Reagents and drugs

3.1.1. Anesthesia

Mice were anesthetized by intraperitoneal injection (i.p.) of 100 mg/kg ketamine (Ketanest® Pfizer Deutschland GmbH, Berlin, Germany) and 10 mg/kg xylazine (Rompun®, Bayer Healthcare, Leverkusen, Germany). After injection mice were set back into their cage and left alone for at least 5 minutes. After 5 minutes depth of anesthesia was controlled by testing paw pinch reflex and rating the breathing frequency. During the experimental procedure mice were continuously observed and depth of anesthesia was assessed every 10 minutes. If necessary anesthesia was prolonged by reinjection. Ketamine and xylazine is often used in mice anesthesia and considered as very reliable [87].

Nevertheless ketamine/xylazine has impact on cardiovascular function. Compared to volatile isoflurane myocardial blood flow is lower in mice anesthetized with ketamine/xylazine [88]. The combination of ketamine/xylazine may decrease heart rate, systolic and diastolic function [89]. Impact on heart rate and left ventricular function is dosage dependent [90]. 100 mg/kg ketamine (Ketanest®) and 10 mg/kg xylazine (Rompun®) is a well approved dosage in laboratory experiments with mice and gives deep anesthesia for C57bl6 and Nrf2 KO mice with only moderate attenuation of cardiovascular function.

Combination of O₂ 100 % and Isoflurane 1.5-2 % was used to maintain anesthesia of mice while echocardiographic assessment (see chapter 3.3.). Depth of anesthesia was controlled and adjusted to breathing rate (100 /min) and heart rate (450-500 bpm) of mice.

3.1.2. Anticoagulation

Before mice were put to death for preparation of isolated hearts mice were heparinized with a single-shot of non-fractional heparin (250 I.U.) together with the injection of anesthetics.

3.1.3. Pharmacological interventions

Adenosine (A9251), bradykinin acetate salt (B3259), 2-ethyl-2-thiopseudourea hydrobromide (ETU) (301310), Ouabain (O3125) and Isoproterenol (Iso) (I2760) (all from Sigma-Aldrich CO LLC, Deisenhofen, Germany) were solved in 0.9 % saline solution. Afterwards bradykinin, adenosine and Iso were diluted with Krebs-Henseleit buffer (see chapter 3.5.) to get the final concentration.

ETU was administered continuously intraperitoneal (1.3 $\mu\text{mol/kg/min}$) via infusion syringe pump while blood pressure was measured. Ouabain bolus (1 nmol/kg) was given i.p. while cardiac contractility was measured. Arterenol solution for injection (Sanofi-Aventis Deutschland GmbH, Frankfurt, Germany) was diluted with 0.9 % saline solution and administered continuously intraperitoneal (40 $\mu\text{g/kg/min}$) via infusion syringe pump while cardiac contractility was measured (see chapter 3.4.).

3.2. Animals

All experiments were approved, accepted and with permission of the regional Government of Germany, Landesamt für Natur, Umwelt und Verbraucherschutz Nordrhein-Westfalen (LANUV) (AZ 84-02.04.2011.A227) according to the European Convention for the Protection of Vertebrate Animals used for Experimental and other Scientific Purposes (Council of Europe Treaty Series No. 123). Animal care and housing was in accordance with the institutional guidelines. The doctoral candidate was educated in the handle and care of experimental animals complying with the regulations of the German Tierschutzgesetz.

Nrf2 KO/C57BL6J (BRC No. 01390) mice were obtained by Riken Bio Resource Center (Koyadai, Tsukuba, Ibaraki, Japan) and crossed for more than 10 generations with C57BL/6J in the Tierversuchsanlage Düsseldorf. For experiments, 5-6 months and 17-18 months old male mice were used. As control, wildtype (WT) littermates were used. If necessary the WT group was stocked up with male C57BL/6J mice bought from Janvier Labs, France. The

bought animals were housed under the same conditions as the Nrf2 KO mice at least for two weeks before experimental begin.

Genotype of each mouse was tested from tail biopsy. Therefore the tip of tail was cut off and lysed within 50 mM sodium hydroxid (NaOH) for 40 minutes at 95°C and bufferd with Tris HCl. Afterwards the KAPPA2G Robust PCR kit (KAPA BIOSYSTEMS, Woburn, Massachusetts, USA) was used to replicate the DNA. Primer (Nrf2 5': TggACgggACTATTgAAggCTg; lacZ: gCggATTgACCGTAATgggATAgg; Nrf2-AS: gCCgCCTTTTCAGTAGATggAgg) were bought by Riken Bio Resource Center (Koyadai, Tsukuba, Ibaraki, Japan). E-Gel® 2 % Agarose by Invitrogen by Life technologies (Carlsbad, California, USA) was used for gel electrophoresis.

3.3. Echocardiographic assessment

Cardiac Imaging was performed with the Vevo 2100 (Visual Sonics Inc., Toronto, Canada) high-resolution ultrasound system (18-38 MHz).

Mice were placed in a small chamber for anesthesia induction with isoflurane and oxygen. When mice lost their consciousness, they were transferred to mask anesthesia on an ECG built-in heating pad. Body temperature was controlled by rectal probe and maintained to 37 °C. ECG was recorded continuously and anesthesia was regulated individually to maintain heart rate of 400 bpm and breathing rate of 100 per minute. All hair was removed from the chest with a common depilatory cream. Water-based ultrasound gel (Aquasonic 100) was applied to the skin for better contact and visibility. Volumes were calculated in b-mode by identification of maximal and minimal cross-sectional area using the manufacturer's analysis software. Doppler ultrasound was applied in apical four-chamber view and mitral inflow was measured. Diastolic function was determined by analyzing the flow profile of mitral valve. Calculated parameters are exemplified in Figure 13. Table 1 and Table 2 explain the obtained parameters.

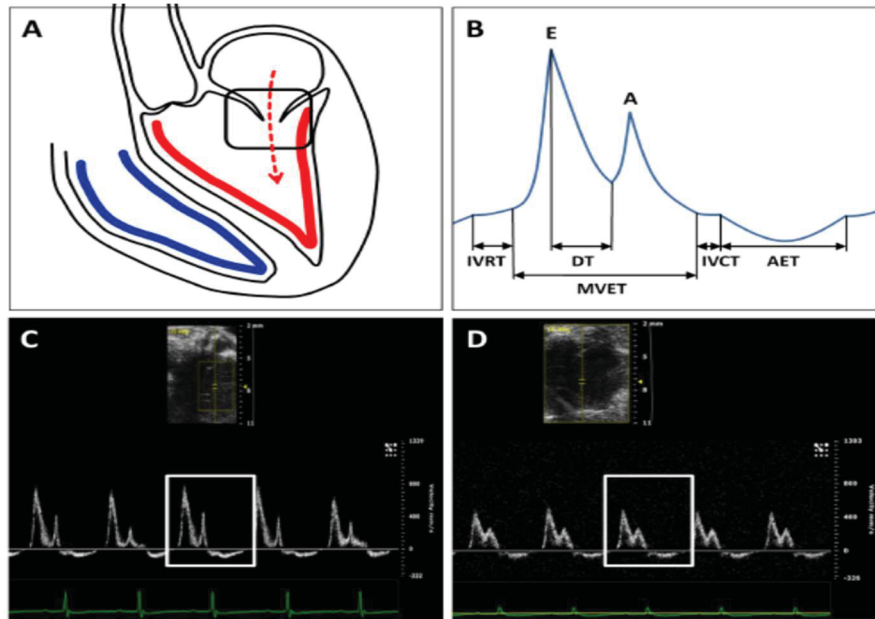


Figure 13: Mitral valve Doppler profile

A) Schematic representation of the blood flow seen in the apical four chamber view. B) Analysis of the mitral valve Doppler profile: Isovolumetric relaxation time (IVRT) and mitral valve ejection time (MVET) represent LV diastole; Isovolumetric contraction time (IVCT) and aortic ejection time (AET) represent LV systole; E-peak (or wave) represents early diastolic filling, followed by the atrial contraction (A-wave); deceleration time of the E-wave (DT) is a commonly used parameter of early diastolic filling assessment. C) and D) representative mitral valve Doppler profile of Nrf2 KO (C) and WT (D) mice. Figure adapted from Erkens et al. [1]

LV-end systolic volume (ESV)	μl	minimal cross-sectional area
LV-end diastolic volume (EDV)	μl	maximal cross-sectional area
stroke volume (SV)	μl	EDV-ESV
ejection fraction (EF)	%	SV/EDV x100
cardiac output (CO)	ml/min	SV x heart rate
fractional shortening (FS)	%	(LVIDd-LVIDs)/LVIDd x100; LVIDd= LV internal diastolic dimension; LVIDs= LV internal systolic dimension
LV mass		left ventricle mass was calculated as: (((1.053x((LVEDD+LVPW, ED+IVS, ED) ³ -LVEDD ³))x0.8) and corrected to body weight

Table 1: Parameters obtained in b-mode parasternal long axis view

E wave	mm/s	first peak of velocity in MV Doppler profile
A wave	mm/s	second peak of velocity in MV Doppler profile
E/A ratio		E wave /A wave
E deceleration time (DT)	ms	time from the maximum of E wave to baseline
mitral valve ejection time (MVET)	ms	total diastolic filling time
aortic ejection time (AET)	ms	total systolic ejection time
isovolumetric relaxation time (IVRT)	ms	time between end of systolic ejection and opening of the mitral valve
isovolumetric constriction time (IVCT)	ms	time between end of diastolic filling and opening of the aortic valve
myocardial performance index (MPI)		(IVRT+IVCT)/ AET

Table 2: Mitral valve Doppler parameters measured in four-chamber view

3.4. Assessment of systemic hemodynamics in vivo (Millar-catheter)

Invasive assessment of systemic hemodynamics was performed with a pressure-conductance catheter (1.4 F Mikro Tip SPR-839, Millar Instrument, Houston, Texas, USA) (Millar catheter) following the closed chest method [91] without intubation.

Mice were anesthetized and placed on a heating pad to control the body temperature. Surgical tape was used to tape down the front paws and hind paws as you can see on Figure 14. Attention was paid to the front paws, which should not be taped with too much pressure because the pressure is transferred to the upper thorax which can affect breathing and further surgical steps. The head was pulled back gently, using a filament around the front teeth to get a better access to operating area and improve breathing by slightly stretching the trachea. A middle-neck incision was done from the mandible to the sternum (Figure 14). The right parotid gland was mobilized bluntly and moved apart (Figure 14). The carotid sheath was dissected carefully and the right common carotid artery (RCCA) was identified and isolated with special attention to not injure the surrounding veins and nerves. Afterwards a ligation was set on the RCCA beneath the bifurcation, pulled gently and taped to the table. A hemostatic clamp (hemostat) was placed as caudal as possible to

prevent loss of blood in the next surgical procedures (Figure 14). A second ligation was placed in the middle between the hemostat and the first ligation with a very loose knot. The RCCA was incised caudal of the first ligation. The incision was pulled softly with a strait microforceps and the Millar catheter tip was inserted into the RCCA. The hemostat was removed and the Millar catheter was pushed carefully forward. The middle suture was gently dragged (Figure 14). The parotid gland was laid back to its physiological position and a soaked swab was covered over it to prevent from further injury and dehydration. For intraperitoneal drug administration a 27 G needle was bended, inserted into the abdomen and connected to a syringe (Figure 14).

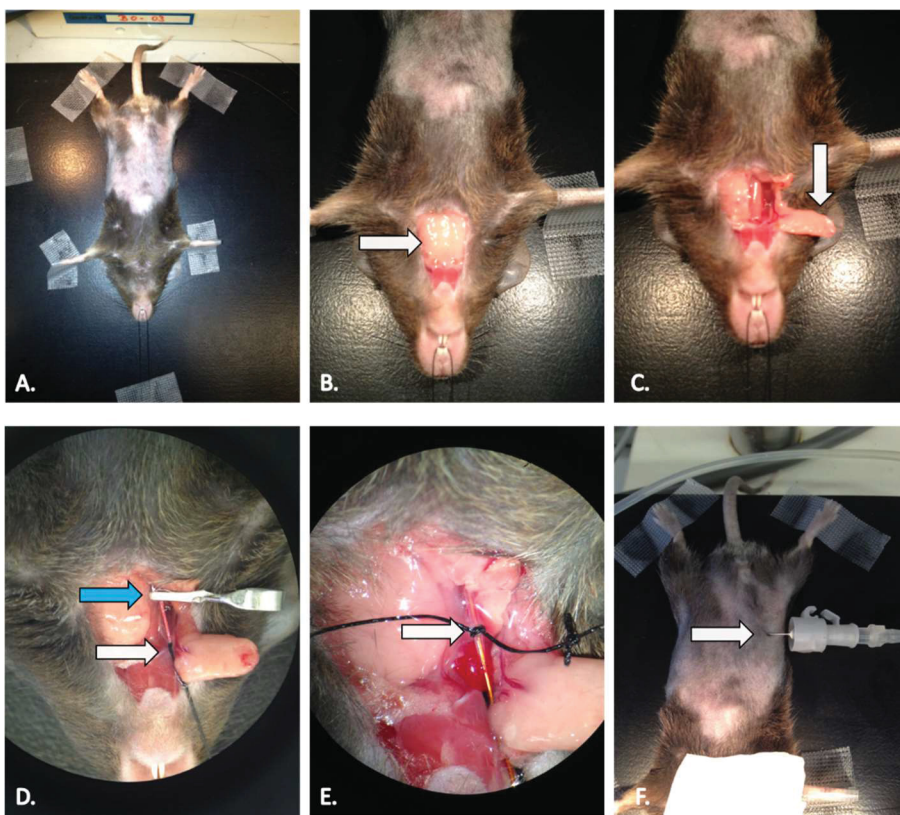


Figure 14: Surgical steps for insertion of Millar catheter

A. Positioning of the mouse on the heating pad. B.+C. sagittal incision of the middle-neck and mobilization of the right parotid gland (white arrow). D. cranial ligation (white arrow) of the isolated RCCA and caudal placement of a hemostat (blue arrow) E. final position of the Millar catheter in the RCCA secured with a suture (white arrow) F. intraperitoneal catheter for drug administration (white arrow).

The Millar catheter was moved into the proximal aorta and a baseline recording was done for at least 2 minutes until a steady pressure signal was recognized. The correct position of Millar catheter was approved by

controlling the shape of the aortic pressure curve which is exemplary shown in Figure 15. One group was treated with ETU ($1.3 \mu\text{mol/kg/min}$) and change of blood pressure was compared to baseline levels.

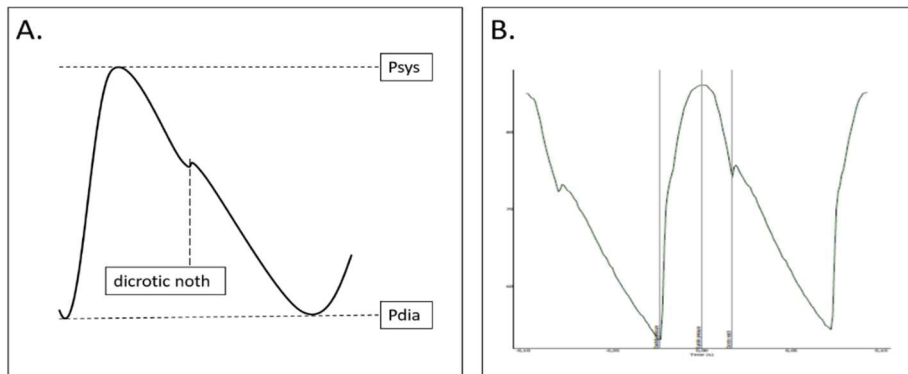


Figure 15: Blood pressure curve

A. Schematic representation of blood pressure curve measured inside the aorta. Shape of which was used to approve the right position of Millar catheter.

B. Representative example of blood pressure curve in Nrf2 KO mice.

After passing the aortic valve, baseline measurement was recorded for another 2 minutes. Position of catheter tip was controlled by the shape of pressure-volume loop (Figure 16). Arterenol or Oubain was injected intraperitoneal and change of pressure parameter were recorded and compared to baseline levels.

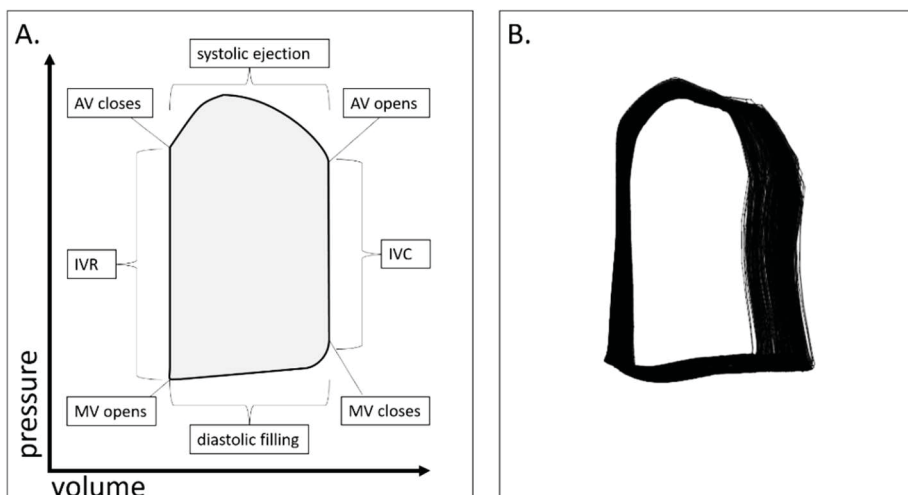


Figure 16: Pressure volume loop

A. Schematic representation of pressure-volume curve measured inside the left ventricle. Shape of which was used to approve the right position of Millar catheter.

AV=aortic valve; MV= mitral valve; IVR= isovolumetric relaxation; IVC= isovolumetric contraction B. Representative example of pressure volume loop in Nrf2 KO mice.

Arterenol (40 µg/kg/min) was injected intra peritoneal with an infusion pump for 12 minutes. Ouabain (1 nmol/kg) was given by intra peritoneal bolus injection. Change of heart parameter was recorded and compared to baseline levels. Mice were divided into 8 groups as described on Table 3. For statistical analyzes of blood pressure and differences in baseline values the groups were pooled from the treatment groups.

Nrf2 KO (6 months old)	n=4	baseline assessment + Arterenol treatment
WT (6 months old)	n=5	baseline assessment + Arterenol treatment
Nrf2 KO (6 months old)	n=7	baseline assessment + Ouabain treatment
WT (6 months old)	n=7	baseline assessment + Ouabain treatment
Nrf2 KO (6 months old)	n=5	blood pressure assessment + ETU treatment
WT (6 months old)	n=5	blood pressure assessment + ETU treatment
Nrf2 (18 months old)	n=6	baseline assessment
WT (18 months old)	n=6	baseline assessment

Table 3: Group design for Millar assessment

The Millar catheter was connected to a Millar Box (Millar, Houston, Texas, USA) and data was recorded and analyzed with LabChart 7 (AD Instruments, Oxford, United Kingdom). Table 4 and Table 5 give an overview of the obtained and calculated values, abbreviations and units.

Psys	mmHg	systolic pressure: peak of pressure measured in the ascending aorta
Pdia	mmHg	diastolic pressure: lowest value of pressure measured in the ascending aorta; diastolic pressure is equal to afterload
Pmean	mmHg	mean pressure measured in the ascending aorta
HR	bpm	heart rate

Table 4: Parameters of blood pressure assessment

PES	mmHg	end-systolic pressure: peak of pressure measured in the left ventricle at the end of systole
PED	mmHg	end-diastolic pressure: left ventricular pressure at the end of diastole; PED represents left ventricular preload
dP/dtmax	mmHg/s	maximum of rate of left ventricular pressure rise: peak value of the derivative of the left ventricular pressure curve; dP/dtmax equals the contractility of the left ventricle because it measures the contraction force over time
dP/dtmin	mmHg/s	minimum of rate of left ventricular pressure decrease: lowest value of the derivative of the left ventricular pressure curve; dP/dtmin equals the lusitropy of the left ventricle because it measures the loss of tension over time
HR	bpm	heart rate
EDV	RVU	End diastolic volume: left ventricular volume at the end of diastole; volume was calculated from conductance and is given in relative volume units
ESV	RVU	End systolic volume: left ventricular volume at the end of systole; volume was calculated from conductance and is given in relative volume units

Table 5: Parameters of in vivo left ventricular pressure volume assessment

3.5. Assessment of cardiac and coronary function ex vivo (isolated perfused heart)

The isolated perfused heart model was first established by Oscar Langendorff 1895 [92]. Since then it has retained its important role for cardiac research [93]. This model gives the possibility to measure coronary flow and myocardial contractility in absence of interferences of the remaining body. This technique allows to compare cardiac and coronary functions of Nrf2 KO and WT mice under constant conditions without systemical differences.

Nrf2 KO mice and WT mice were anesthetized and heparinized. Afterwards they were killed by cervical dislocation and the heart was removed as fast as possible by thoracotomy. For that it was done a vertical incision of 1 cm below the xiphoid. To open the thorax the xiphoid was slightly lifted with an anatomically curved forceps and the diaphragm was incised. Bilateral cuts in cranial direction were performed severing the ribs. The ventral part of the thorax was deflected with caution to enable good view of heart and lungs. The mediastinum, heart and lungs were removed by severing the aorta descendens and the vena cava and cutting along the spine from caudal to cranial. Thereby the small thoracic vessel branches were cut off.

The mediastinum, heart and lungs were placed immediately on a 4 °C cold dissect dish which was filled before with heparinized and oxygenised Krebs-Hanseleit solution to facilitate heart preparation in a nutrient- and oxygen-rich liquid. With help of an optical microscope lungs, thymus, trachea and oesophagus were removed and aorta and heart were isolated. Aorta was cut off just proximal the brachiocephalic trunk. Pulmonary veins were cut off to get access to the left atrium to place a balloon in the left ventricle later on. The aorta was then cannulated and fixed to a 21 gauge stainless steel needle, which was filled before with heparinized Krebs-Henseleit-buffer to avoid air bubbles.

The needle was set to the Langendorff perfusion rig (Apparatus Isolated Heart by Hugo Sachs Elektronik, March-Hugstetten, Germany) as shown on Figure 17.

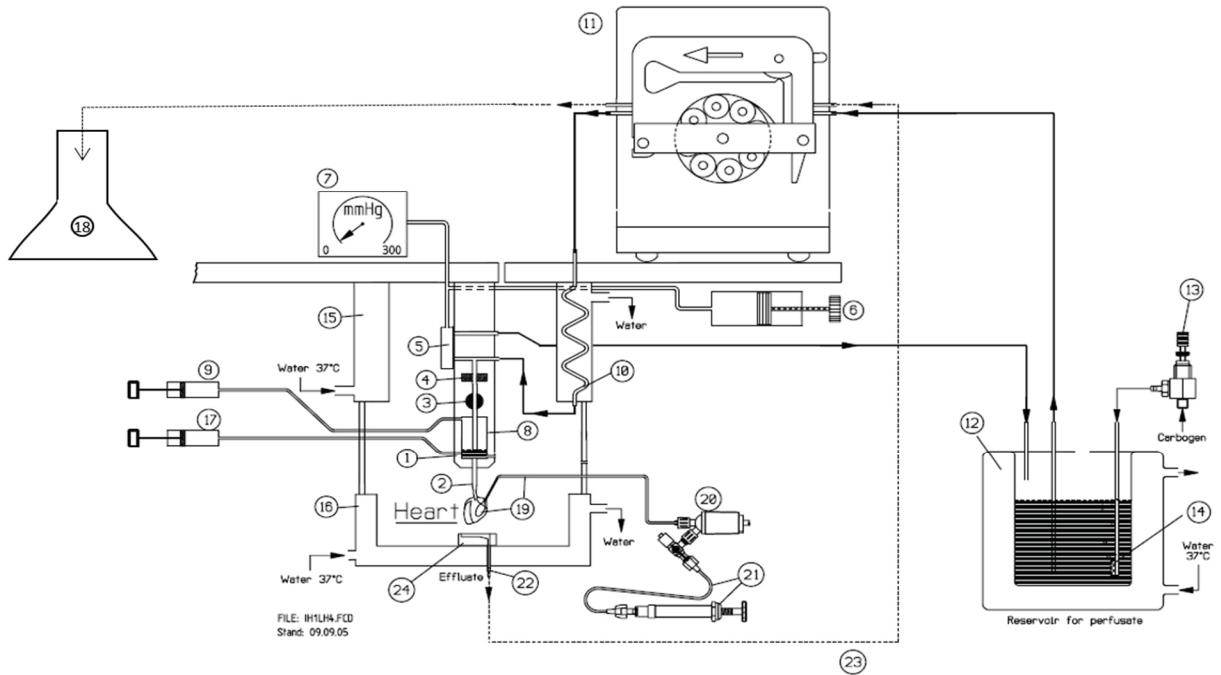


Figure 17: Apparatus Isolated Heart

Modified Drawing adapted by and with approval of Hugo Sachs Elektronik, March-Hugstetten, Germany [94]

The aorta is cannulated with a needle (2) which is set to the aorta block (1), which is supplemented with the flow probe (4) and the stopcock block (3). Warm perfusate is pumped (11) from the reservoir (12) into the air vessel (8). Constant perfusion pressure is set to 100 mmHg (7) by adjusting the membrane (5) with a big syringe (6). Drugs are administered directly into the aorta block (17). Left-ventricular pressure is measured (20) with a small waterfilled ballon (19) inside the left ventricle. Preload was adjusted (21) to 10 mmHg. The effluante is not recirculated (23) but disposed (18).

(9) Syringe for adjusting the air volume in the air vessel; (10) Metal heat exchanger; (13) carbogen gas; (14) gas frit; (15) Upper part of the jacketed heart chamber, thermostated by water circulator; (16) Lower part of the jacketed heart chamber, thermostated. The lower part can be swung away downwards to have access to the heart; (18) Pressure transducer; (22) Discharge tube; (24) Effluante funnel to collect effluante dropping down from the heart

A constant perfusion pressure was set to 100 mmHg. Then a water filled balloon was inserted through mitral valve via the left atrium into the left ventricle. The balloon was connected to a pressure transducer and a syringe to set a constant preload of 10 mmHg. Then a pacer was connected and set to 600 beats per minute. The isolated heart was perfused with modified Krebs-Henseleit-Buffer NaCl (118 mM), KCl (4.7 mM), MgSO₄ (0.8 mM), NaHCO₃ (25

mM), KH_2PO_4 (1.2 mM), Glucose (5 mM), Pyruvic acid (1.9 mM) and CaCl_2 (2.5 mM) bubbled with carbogen gas (95 % O_2 and 5 % CO_2). Temperature of the isolated heart was controlled by a common pyrometer and daily taken samples of the buffer confirmed pH 7.4.

Table 6 gives an overview of the obtained and calculated values. The parameters were measured by using an analog-digital converter (2000 Hz) and dedicated software. Data was recorded with IOX 2.2 (EMKA technologies, Paris, France) and analyzed with Microsoft Excel.

Flow	ml/min	rate of flow through the coronary arteries
perfusion pressure	mmHg	constant pressure applied on the aorta by retrograde perfusion; perfusion pressure is equal to afterload and was set to 100 mmHg
PED	mmHg	end-diastolic pressure: left ventricular pressure at the end of diastole; PED represents left ventricular preload and was set to 10 mmHg
PES	mmHg	end-systolic pressure: left ventricular pressure at the end of systole;
DP	mmHg	developed pressure = systolic pressure – diastolic pressure
dP/dtmax	mmHg/s	maximum of rate of left ventricular pressure rise: peak value of the derivative of the left ventricular pressure curve; contraction force over time; dP/dtmax is considered as the contractility
dP/dtmin	mmHg/s	minimum of rate of left ventricular pressure decrease: lowest value of the derivative of the left ventricular pressure curve; loss of tension over time; dP/dtmin is considered as the lusitropic state
HR	bpm	heart rate paced to 600 bpm, physiologic heart rate of mice

Table 6: Parameters obtained ex vivo in isolated hearts

Hearts of 6-months old Nrf2 KO (n=14) and WT (n=15) mice and 18 months old Nrf2 KO (n=10) and WT (n=8) mice were isolated and exposed to the experimental protocol, which is shown in Figure 18. One minute of preliminary recording was used to check the consistent coronary flow and left ventricular pressure. Then stabilization period of 20 minutes was given until the heart showed a steady coronary flow and a constant developed pressure.

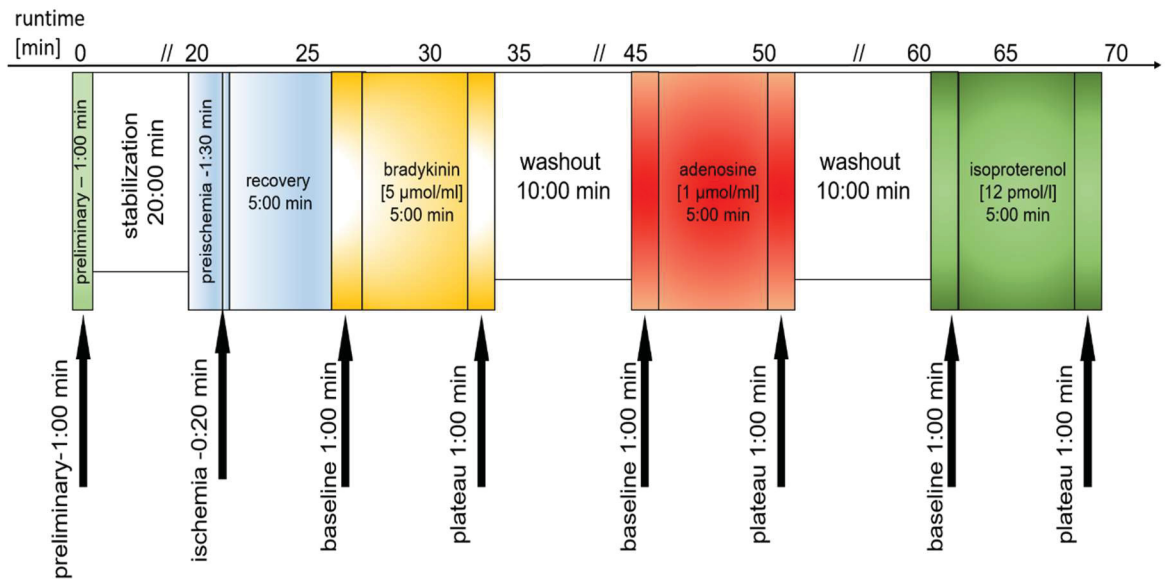


Figure 18: Langendorff experimental procedure

Flow and contractility after short-time ischemia (blue), bradykinin-(yellow), adenosine-(red) and isoproterenol- (green) administration was recorded. Before each administration 1 minute baseline recording was performed. Between the drug administration 10 minutes washout was performed.

Then flow was interrupted for 20 seconds followed by 5 minutes of reperfusion. This hyperemic response to short time ischemia is generally accepted as a valid evaluation of coronary flow reserve. Afterwards, bradykinin 5 μmol/ml, adenosine 1 μmol/ml and isoproterenol 12 pmol/l were added to the aortic cannula one after another with 10 minutes washing period in between. Increase of coronary flow was recorded and compared to baseline level after infusion of bradykinin and adenosine. Increase of DP, dP/dtmax, dP/dtmin and heart rate were recorded and compared to baseline levels after administration of Iso. To enhance reliability only hearts fulfilling the criteria shown in Table 7 were used.

preparation time was under 10 minutes
preliminary developed pressure was over 100 mmHg and flow was over 5 ml/min
hyperemic response to short ischemia (20 seconds) revealed in an increase of flow at least 150 % compared to baseline
flow and developed pressure were not dropping down rapidly during experimental procedure

Table 7 exclusion criteria for isolated perfused hearts

3.6. Statistical analyses

The results are given as mean \pm standard error of the mean (SEM). Statistical significance was analyzed by 1-way ANOVA and followed by Bonferroni post hoc comparison. If only two groups were tested unpaired t-test was applied. Normal distribution was tested by D'Agostino-Pearson test. $p < 0.05$ was considered as statistically significant.

4. Synopsis of pharmacological approach to study vascular and cardiac function

To analyze coronary function of Nrf2 KO mice adenosine and bradykinin were administered and increase of coronary flow was recorded.

4.1 Adenosine

Adenosine is endogenous and plays a ubiquitous role in cell signaling not only in the cardiovascular system but nearly in every organ in the body [18]. Four subtypes of receptors are known for adenosine [18]: A_1 -, A_{2A} -, A_{2B} - and A_3 -receptor (Figure 19). All of them are G-protein coupled receptors. Extracellular adenosine activates one of the receptors. The α -subunit releases GDP which allows GTP to bind instead. This leads to a dissociation of the G-protein-complex into the α -subunit and the $\beta\gamma$ -subunit. The $\beta\gamma$ -subunit regulates gene expression in context with cell growth and remodeling.

A_1 -receptor and A_3 -receptor are α_i -protein coupled, which inhibits the adenylate cyclase activity. A_{2A} - and A_{2B} -receptor are associated to α_s -subunit stimulating adenylate cyclase and modifying Ca^{2+} handling. As A_1 and A_3 receptors can be considered as antagonist to A_{2A} and A_{2B} receptors, the downstream reaction of adenosine varies from tissue to tissue dependent of the receptor pattern. Different studies have assessed the effect of adenosine for the cardiovascular system. Physiological heart function requires a balance between A_1 and A_{2A} receptors [95]. It has been shown that overexpression of

A_1 -receptor is associated with hypertrophy and bradycardia, whereas overexpression of A_{2A} -receptor leads to faster heart rates and is cardioprotective in pressure-overloading situations but is not cardioprotective in general [95].

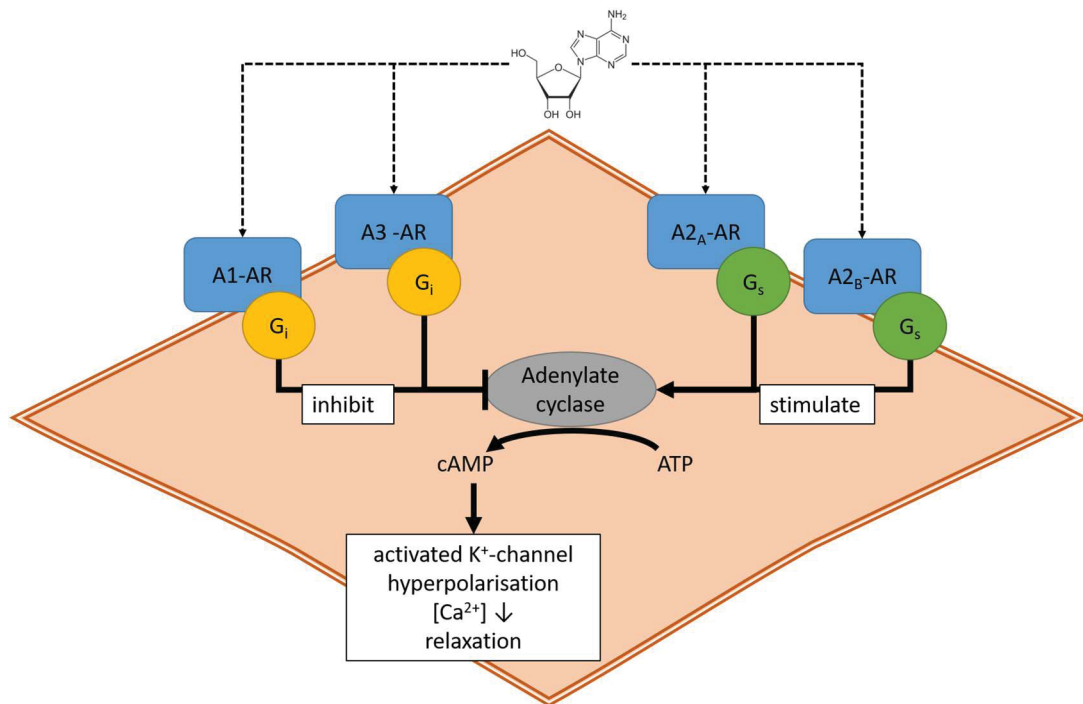


Figure 19: Adenosine receptors

A_1 -AR and A_3 -AR are G_i -protein coupled receptors, which inhibit the synthesis of cAMP. A_{2A} -AR and A_{2B} -AR are G_s coupled stimulating adenylate cyclase activity and relax the VSMC endothelium independently.

Referring to Berne's adenosine hypothesis [96], physiologically adenosine is released by cardiac myocytes in case of hypoxia to activate adenosine-receptors on the surface of smooth muscle cells [17]. This causes vasodilation and hereby (re-)increases the myocardial pO_2 [97]. In smooth muscle cells increased levels of cAMP, following A_{2A} -receptor stimulation, lead to vasorelaxation [98].

Besides direct stimulation of smooth muscle cells, there is also evidence that endothelial A_{2A} -receptors stimulate endothelial NO release [99], whereas A_1 -receptors might decrease NO release [100] (Figure 20).

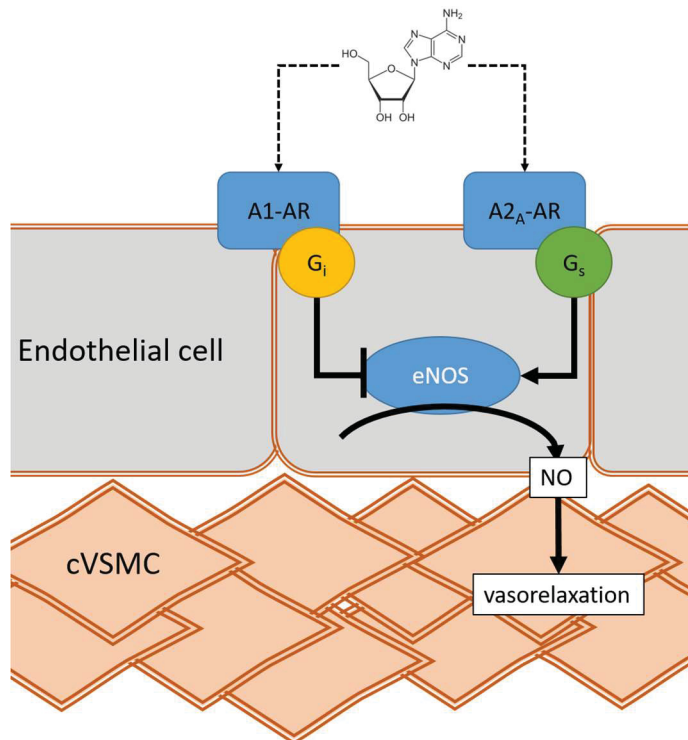


Figure 20: Endothelium dependent vasodilation of adenosine

Endothelium dependent vasorelaxation of adenosine is dependent of the adenosine receptor pattern of the endothelial surface. Stimulation of A_{2A}-AR may activate eNOS and NO is released. NO diffuses to coronary vascular smooth muscle cells (cVSMC) and causes relaxation.

Recently it is proposed that ROS mediate the vasodilatory response to adenosine [101-104]. Binding to A_{2A}-AR leads to activation of NADPH oxidase (Nox). Nox generates O₂⁻ which is then converted to H₂O₂. H₂O₂ is able to relax vascular smooth muscle cells [101, 105] by diffusing into them and activating K_{ATP} channels. K_{ATP} channels hyperpolarize vascular smooth muscle cells and lead to vasodilation. It has been shown that inhibition of Nox attenuates vasodilation after adenosine treatment [104].

A₁-AR deficient mice have a higher magnitude of adenosine induced H₂O₂ production [102] and a higher vasodilation suggesting that A₁-AR antagonizes A_{2A}-AR-induced-H₂O₂-mediated vasorelaxation (Figure 21).

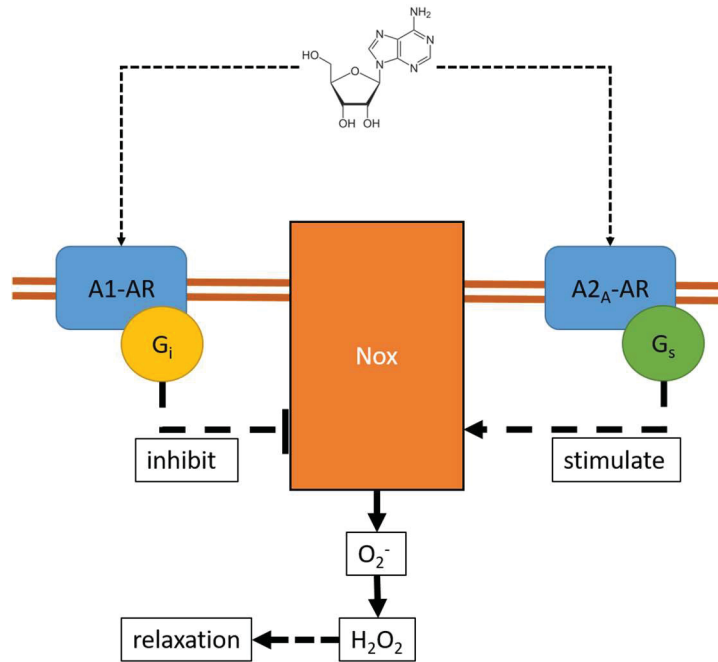


Figure 21: H₂O₂ mediated adenosine response

A₁-AR may inhibit NADPH oxidase (Nox) and A_{2A}-AR may stimulate Nox resulting in H₂O₂ generation, which may hyperpolarize VSMC and result in vasodilation. [101-104]

4.2 Bradykinin

The endogenous endothelium-dependent vasodilator bradykinin consists of nine amino-acids. Bradykinin is part of the kinin-kallikrein-system and generated out of high-molecular-weight kininogen by kallikrein. Bradykinin serves multiple functions such as vasodilation or proinflammatory response and plays a role in chronic pain [106]. Bradykinin is degraded by several amino- and carboxypeptidases including angiotensin converting enzyme (ACE) [107].

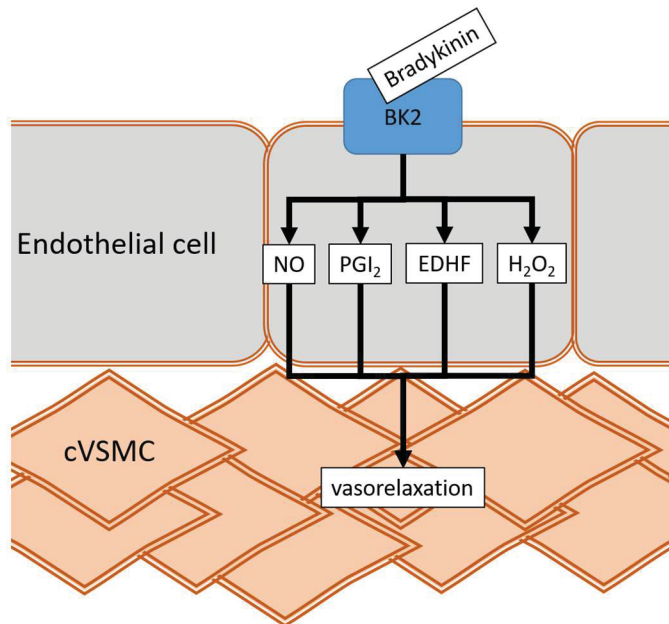


Figure 22: Vascular bradykinin response

On the surface of endothelial cells BK2 is the predominantly expressed bradykinin receptor. Its stimulation releases vasodilatory factors which are able to relax coronary vascular smooth muscle cell (cVSMC).

PGI₂=Prostaglandin I₂; EDHF=endothelium-derived hyperpolarization factor;

Two receptors are classified for Bradykinin, BK1- and BK2-receptor both are G-protein coupled. Cardiovascular research has focused on BK2 receptor. Its stimulation is well known to cause coronary dilation. Whereas BK1-receptor is in the focus of studies on tissue injury and inflammation. However there is also evidence for BK1-receptor involvement in coronary hyperemic response [108].

BK2-receptor is constitutively expressed on endothelial cells. It causes vasodilation (Figure 22) by stimulating the endothelium to release prostacyclin, endothelium-derived hyperpolarizing factor (EDHF), H₂O₂ and NO [109-112]. In isolated perfused hearts bradykinin is often used to assess endothelium dependent coronary vasorelaxation. One of the most important pathways of endothelium dependent vasorelaxation is the production of NO by eNOS [111, 112].

4.3 2-ethyl-2-thiopseudourea

2-ethyl-2-thiopseudourea (ETU) (1.3 $\mu\text{mol/kg/min}$) was administered to increase blood pressure in vivo. ETU is a specific NOS inhibitor. Therefore ETU was used to evaluate the contribution of eNOS to the total vascular resistance. Endothelial NOS is activated by multiple stimuli such as shear stress or bradykinin.

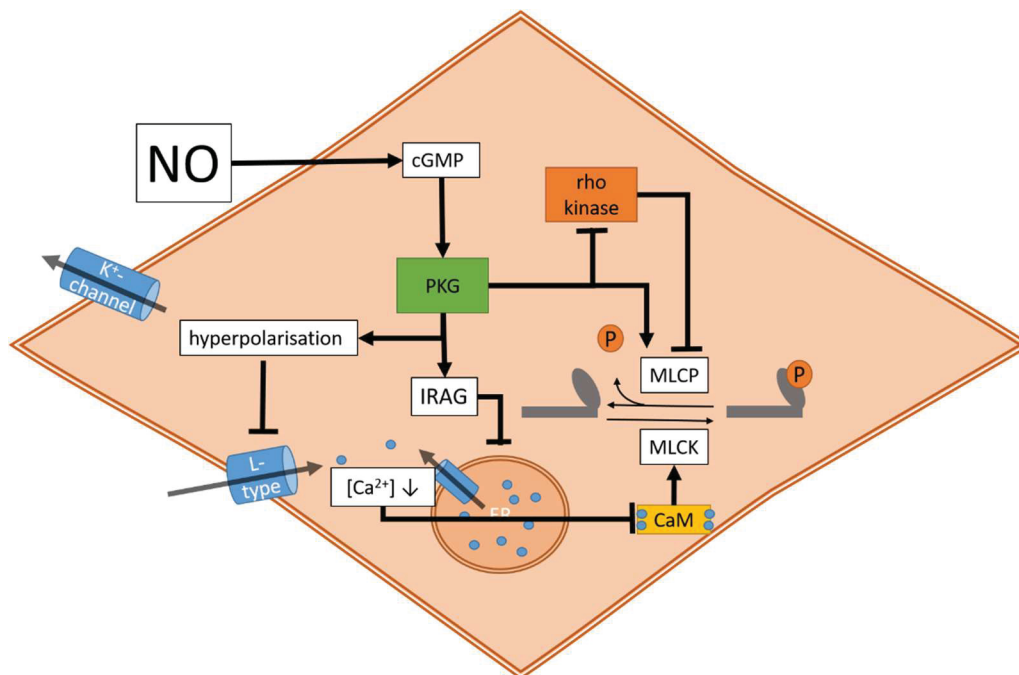


Figure 23: NO mediated vasorelaxation

Nitric oxide is able to diffuse into VSMC and stimulate the generation of cyclic guanosine monophosphate (cGMP) which activates protein kinase G (PKG). PKG directly stimulates myosin light chain phosphatase (MLCP), inhibits rho kinase and reduces the cytoplasmic Ca^{2+} concentration by inhibiting the endoplasmic Ca^{2+} release and Ca^{2+} influx from extracellular. PKG activates IP3 receptor-associated cGMP kinase substrate (IRAG) which decreases endoplasmic Ca^{2+} release. PKG activates K^+ -channels which hyperpolarize the cell and decreases open probability of L-type Ca^{2+} channels. Intracellular Ca^{2+} concentration is needed to activate calmodulin. Thus decreased Ca^{2+} concentration is inhibiting myosin light chain kinase (MLCK).

eNOS catalyzes the oxidation from L-arginin to L-citrullin to generate NO. NO diffuses to vascular smooth muscle cells and activates NO sensitive guanylyl cyclase. NO sensitive guanylyl cyclase generates cGMP which is responsible for smooth muscle cell relaxation (Figure 23). Inhibition of eNOS by ETU causes vasoconstriction. Intraperitoneal administration of ETU increases vascular resistance and hereby increases cardiac afterload which results in an increase of blood pressure.

4.4 Isoproterenol and arterenol

Isoproterenol (Iso) is a synthetic derivative of endogenous adrenaline. It is a non-selective agonist of adrenergic receptors, with a high affinity to beta-adrenergic receptors (β -AR) and lower affinity to alpha adrenergic receptors (α -AR) [113]. Arterenol, which is also called noradrenaline or norepinephrine, is an endogenous catecholamine with higher affinity to α -AR and lower affinity to β -AR [113]. All adrenergic receptors are G-protein coupled receptors. Their ubiquitous expression is necessary to enable the sympathetic “flight or fight” response. β -AR are linked to G_s -protein and activation of β -AR leads to an increase of cAMP and activation of protein kinase A (PKA). PKA is responsible for most of the downstream effects of isoproterenol.

β -AR can be classified into β_1 -AR, β_2 -AR and β_3 -AR. β_1 -AR is highly expressed on cardiac cells. Activation of β_1 -AR leads to positive inotropic, positive chronotropic, positive lusitropic, positive dromotropic and positive bathmotropic response [14, 114]. β_2 -AR can be found on the surface of smooth muscle cells in coronary arteries, the lungs and the gastrointestinal tract. Its activation causes smooth muscle relaxation, leading to vasodilation of coronary arteries, bronchodilation and rest of degustation. β_3 -AR are expressed on adipocytes and increase lipolysis [14, 114].

α -AR are classified into α_1 -AR and α_2 -AR. α_1 -AR is G_q -protein coupled and α_2 -AR is linked to G_i -protein [14, 114]. α_1 -AR is expressed on the surface of smooth muscle cells. Dissociation of the G_q -protein activates phospholipase C (PLC) and enhances IP_3 and Ca^{2+} concentration leading to contraction of smooth muscle cells [114]. High expression of α_1 -AR is found in vascular smooth muscle cells of the skin and GIT and smooth muscle cells of the uterus, ureter and sphincter muscles. α_2 -AR is linked to G_i -protein. G_i -protein inhibits adenylate cyclase and hereby decreases intracellular cAMP. In the central nervous system and at prejunctional terminals α_2 -AR is a presynaptic autoreceptor inhibiting further release of norepinephrine by negative feedback [114].

4.5 Ouabain

Ouabain was used to increase cardiac contractility. Ouabain, also known as g-strophantin, belongs to the family of cardiac glycosides. It can be found in some native plants of eastern Africa, and its toxic effect has been traditionally used as arrow poison. Ouabain is an inhibitor of the Na⁺-K⁺-ATPase and has been used in therapy of heart failure and atrial fibrillation [115]. Cardiac glycosides are known to increase cardiac contractility and in long-term use decrease heart rate. Nowadays the clinical use of cardiac glycoside is very limited because studies failed to verify a decrease in mortality of patients treated with cardiac glycosides [116]. Today's therapeutically use of ouabain in human medicine is uncommon but it is still used in cardiovascular research [115]. Recently endogenous molecules with ouabain-like effect have been found and it is controversial whether this "endogenous ouabain" has significant contribution to cardiovascular homeostasis and if its structure is similar to the ouabain synthesized of plants [117].

5. Results

5.1. Systemic hemodynamics of Nrf2 KO mice

To determine whether lack of Nrf2 affects systemic hemodynamics, Nrf2 KO and WT mice were analyzed by pressure-conductance catheter in the ascending aorta. Nrf2 KO mice showed a significantly lower blood pressure compared to wildtype littermates (Table 7). Systolic and diastolic pressure were about 15 mmHg lower in Nrf2 KO. There were no differences in heart rate, nor in duration or shape of the pressure curves.

To investigate whether the hemodynamics of Nrf2 KO mice changes with age, 18 months old WT and Nrf2 KO mice were measured with Millar catheter. Neither old Nrf2 KO nor WT mice showed significant differences in blood pressure compared to 6 months old mice (Figure 24).

Blood Pressure	WT 6 months old n=17	Nrf2 KO 6 months old n=16
Systolic Pressure (mmHg)	88.54* (± 9.79)	72.63* (± 6.59)
Diastolic Pressure (mmHg)	56.77* (± 9.38)	43.59* (± 7.61)
Mean Pressure (mmHg)	72.75* (± 9.89)	57.42* (± 7.52)
Heart Rate (BPM)	610.74 (± 58.11)	576.68 (± 55.67)

Table 8: Blood pressure of young Nrf2 KO mice

Measured with pressure conductance catheter in ascending aorta.

(*p<0.05; unpaired t-test)

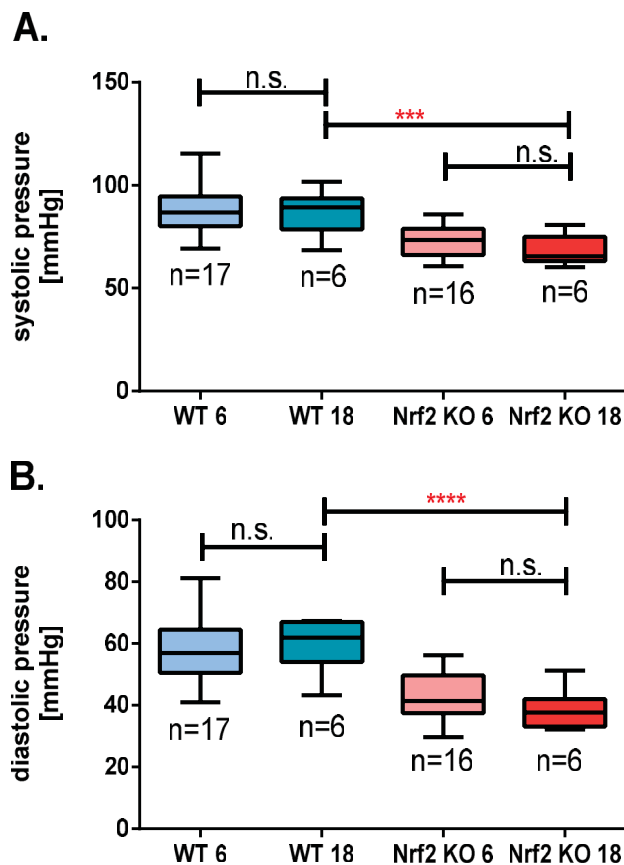


Figure 24: Blood pressure of young and old Nrf2 KO and WT mice

Aortal systolic pressure (A.) and diastolic pressure (B.) were not significantly different in 18 months old mice compared to their 6 months old littermates of equal genotype. 18 months old WT mice had significantly higher blood pressure than 18 months old Nrf2 KO mice. (n.s. not significant; ***p<0.001; ****p<0.0001; 1-way ANOVA, Bonferroni post-hoc)

ETU (1.3 $\mu\text{mol/kg/min}$) was administered intra peritoneal to evaluate the contribution of eNOS to total vascular resistance of Nrf2 KO and WT mice. As described in Table 9 there were no significant differences in blood pressure after administration of ETU.

Blood Pressure	WT n=5	Nrf2 KO n=5
Systolic Pressure (mmHg)	134 (± 12)	122 (± 31)
Diastolic Pressure (mmHg)	96 (± 15)	85 (± 24)

Table 9: Blood pressure after administration of ETU

Systolic and diastolic pressure were not significantly different after administration of ETU. (unpaired t-test, $p < 0.05$)

Lack of Nrf2 decreases blood pressure which leads to the question why there is such a difference. Arterial blood pressure (MAP) is dependent of cardiac output (CO) and systemic vascular resistance (SVR) according to the equation $\text{MAP} = \text{CO} \times \text{SVR}$ (see chapter 1.1). Therefore, it was necessary to analyze the vascular and the cardiac function separately.

5.2. Cardiac function of Nrf2 KO mice

To determine the effect of Nrf2 deficiency on cardiac function, Nrf2 KO mice and WT mice were assessed in vivo by echocardiography and pressure conductance catheter and ex vivo by using the isolated heart model.

Echocardiographic assessment of 6 months old Nrf2 KO mice showed normal systolic function and unaltered cardiac output. Hearts of Nrf2 KO mice showed LV hypertrophy determined in an increased LV mass to body weight ratio (Table 10).

Diastolic function measured by analyzing the Doppler flow profile of mitral inflow was significantly altered in Nrf2 KO mice compared to WT littermates.

Prolonged DT, prolonged MVET and IVRT and increased MPI show that LV relaxation is prolonged in Nrf2 KO mice. E/A ratio was significantly increased in Nrf2 KO mice indicating impaired diastolic filling (Figure 25).

Echocardiography	WT 6 months old n=10	Nrf2 KO 6 months old n=12
Stroke volume (μl)	30.6 (± 5.3)	35.8 (± 6.8)
Ejection fraction (%)	50.1 (± 9.3)	41.4 (± 7.7)
Fractional shortening (%)	10.2 (± 3.2)	10.8 (± 4.4)
Heart Rate (bpm)	393 (± 20.7)	372 (± 22.5)
Cardiac Output (ml/min)	13.1 (± 2.7)	13 (± 2.6)
Endsystolic volume (μl)	32.8** (± 9.8)	54.5** (± 17.2)
Enddiastolic volume (μl)	63.6** (± 10.1)	90.3** (± 20.8)
LV Mass corrected (mg)	69.7 (± 15.2)	88.6 (± 17.1)
LVM/BW (mg/g)	1.98* (± 0.34)	2.71* (± 0.58)

Table 10: Echocardiographic assessment of Nrf2 KO mice

Left ventricular assessment of 6 months old Nrf2 KO mice compared to littermates. Systolic function was not significantly different to WT mice. Endsystolic and enddiastolic volume was significantly higher in Nrf2 KO mice. Left ventricular mass to body weight ratio (LVM/BW) was significant higher in Nrf2 KO mice.
(unpaired t-test, * p<0.05; **p<0.01)

In-vivo measurements of the left ventricle pressure volume conditions with Millar catheter confirmed that end systolic pressure was significantly lower in mice lacking Nrf2 compared to littermates. HR, volume, cardiac output, dp/dtmax and dp/dtmin were the same in both groups (Table 11).

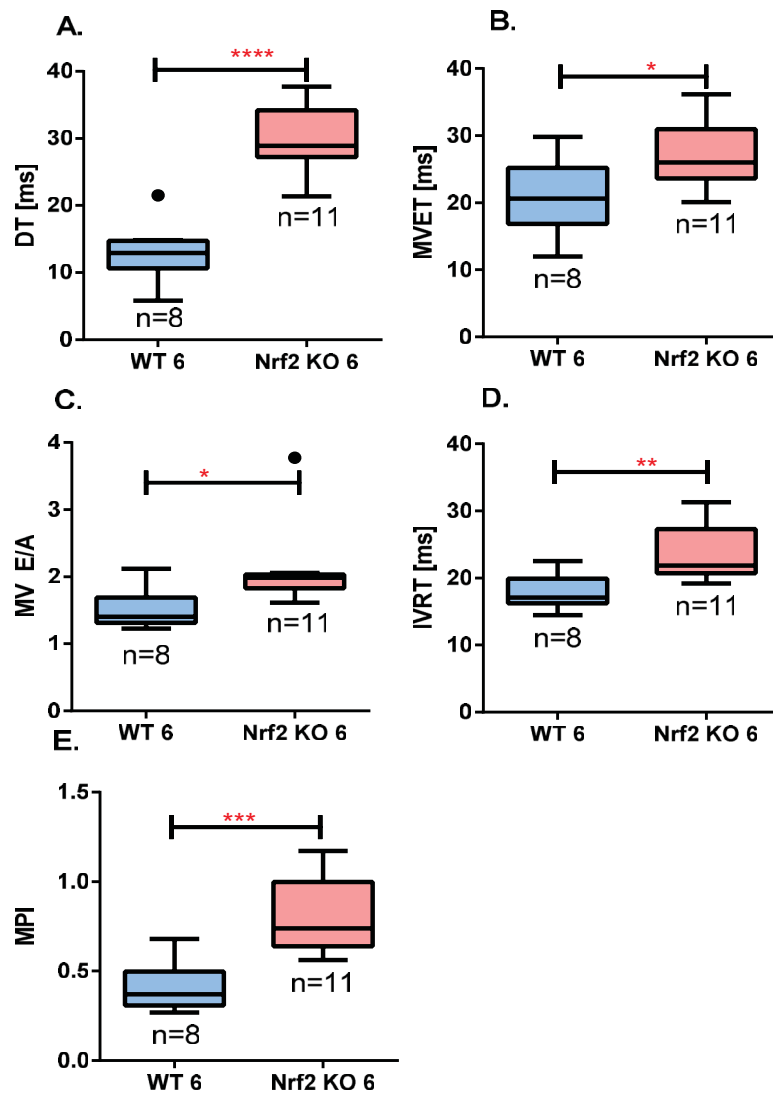


Figure 25: Diastolic function of young Nrf2 KO mice

Echocardiographic assessment of mitral valve Doppler profile of 6 months old Nrf2 KO mice compared to same aged littermates. Left ventricular relaxation is significantly prolonged in Nrf2 KO mice shown in increased deceleration time (DT) (A), increased total diastolic filling time (MVET) (B), increased E/A ratio (C), increased isovolumic relaxation time (IVRT) (D) and increased myocardial performance index (MPI) (E).

(Unpaired t-test * p<0.05; ** p<0.01; *** p<0.001; **** p<0.0001)

Millar Heart Baseline	WT 6 months old n=12	Nrf2 KO 6 months old n=11
CO (RVU/min)	2702 (± 721)	2799 (± 1429)
Endsystolic volume (RVU)	16.59 (± 1.02)	17.81 (± 1.62)
Enddiastolic volume (RVU)	19.28 (± 1.79)	20.31 (± 2.58)
PES (mmHg)	84.05* (± 5.52)	77.03* (± 7.71)
Heart rate (bpm)	609 (± 50.27)	599 (± 60.59)
dP/dt max (mmHg/s)	12717 (± 2808)	11800 (± 3247)
dP/dt min (mmHg/s)	10457 (± 2208)	-9762 (± 1820)

Table 11: LV-pressure-volume relationship in Nrf2 KO mice

RVU= relative volume units calculated from conductance (*student t-test; p<0.05)

The administration of Arterenol increased LV contractility in both genotypes (Table 12). This was shown in an increase of PES, dP/dtmax and HR. Nrf2 KO mice had a lower increase of contractility, whereas the increase of HR was not significantly different (Figure 26).

Millar Heart + Arterenol	WT 6 months old n=5	Nrf2 KO 6 months old n=4
CO (RVU/min)	3797 (± 1073)	4177 (± 1028)
Ves (RVU)	14.5 (± 1)	17.81 (± 2.5)
Ved (RVU)	18.9 (± 1.4)	22.8 (± 2)
PES (mmHg)	106.3* (± 13)	91.7* (± 7)
HR (bpm)	682 (± 29)	629 (± 58)
dP/dt max (mmHg/s)	23980* (± 3264)	18310* (± 4419)
dP/dt min (mmHg/s)	-11483 (± 2568)	-10733 (± 2176)

Table 12: LV- pressure-volume relationship after Arterenol administration

RVU = relative volume units calculated from conductance (*students t-test; p<0.05)

In wildtype mice end systolic and diastolic volume decreased while ejection fraction and stroke volume increased whereas in Nrf2 KO mice volume was not affected. Cardiac output increased to the same extent in both groups.

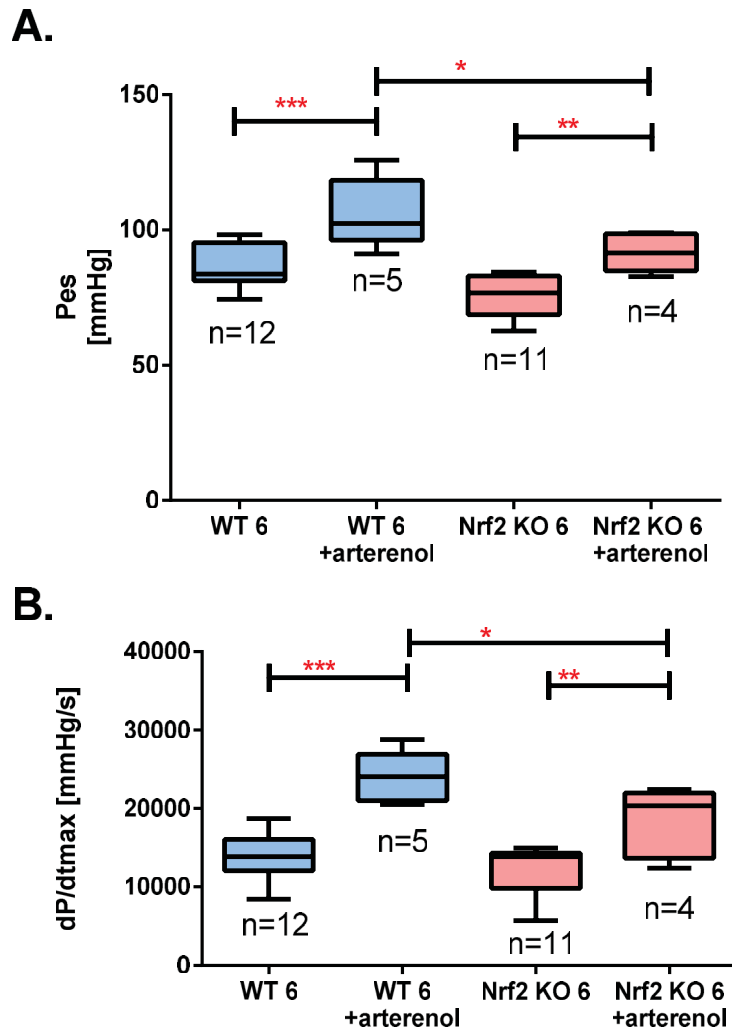


Figure 26: LV-contraction baseline and after Arterenol treatment

End-systolic pressure (A.) and dP/dtmax (B.) increased significantly more in WT than in Nrf2 KO mice. (*p<0.05; **p<0.01; ***p<0.001; 1-way ANOVA, Bonferoni post-hoc)

12-20 minutes after Ouabain treatment (1 μ mol/g) WT mice responded with an increase of dP/dtmax and PES, whereas volume and HR did not significantly change. Nrf2 KO mice showed no significant increase of dP/dtmax. Although PES increased, it did not reach the extent of WT mice (Figure 27).

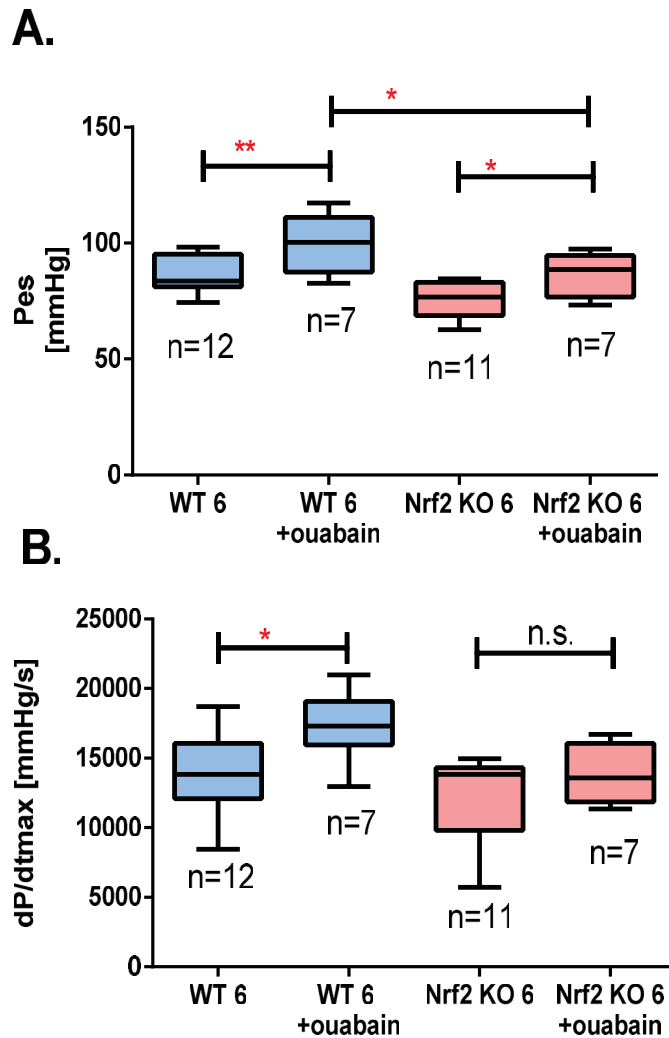


Figure 27: LV- contractility baseline and after ouabain treatment

End-systolic pressure increased significantly more in WT mice than in Nrf2 KO mice after ouabain treatment (A.). DP/dtmax (B.) increased in WT mice after ouabain administration but not in Nrf2 KO mice. (*p<0.05; **p<0.01; n.s. not significant; 1-way ANOVA, Bonferoni post-hoc)

The observed differences in Millar catheter could be mediated by vascular resistance. To determine cardiac function without systemical interference isolated hearts of Nrf2 KO and WT mice were analyzed. Under baseline conditions (preload 10 mmHg) there were no differences in contractility detectable between isolated hearts of Nrf2 KO and WT mice. After stimulation with Iso all hearts responded with an increase of developed pressure, dP/dtmax and dP/dtmin. Nrf2 deficient mice showed a significantly reduced

increase of developed pressure, dP/dtmax and dP/dtmin compared to WT littermates (Figure 28).

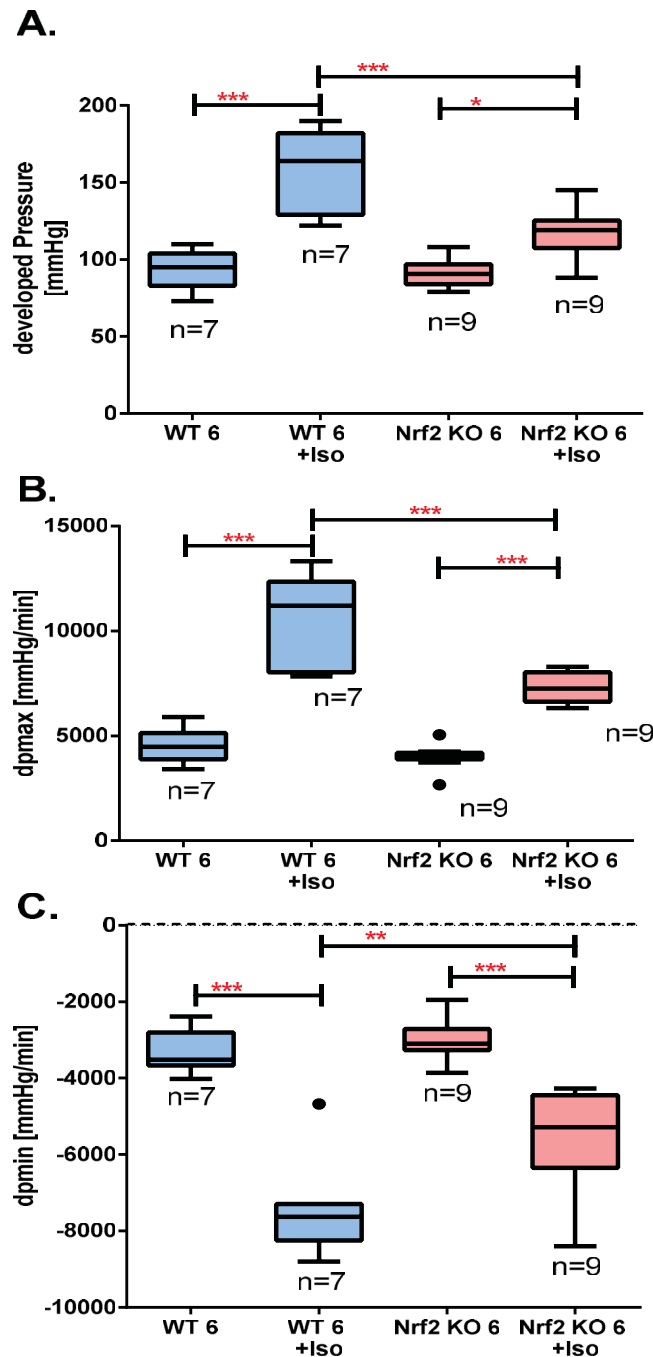


Figure 28: Contractility of isolated hearts of 6 months old mice

Developed pressure (A.), dP/dtmax (B.) and dP/dtmin (C.) of isolated hearts of 6 months old Nrf2 KO and WT mice were analyzed. After administration of Iso contractility increased in both genotypes. Response to Iso was significantly higher in WT mice.

(*p<0.05; **p<0.01; ***p<0.001; 1-way ANOVA, Bonferoni post-hoc)

To see if aging affects impaired cardiac function of Nrf2 KO mice isolated hearts of 18 months old Nrf2 KO and WT mice were analyzed and compared to their 6 months old littermates (Figure 29, Figure 30).

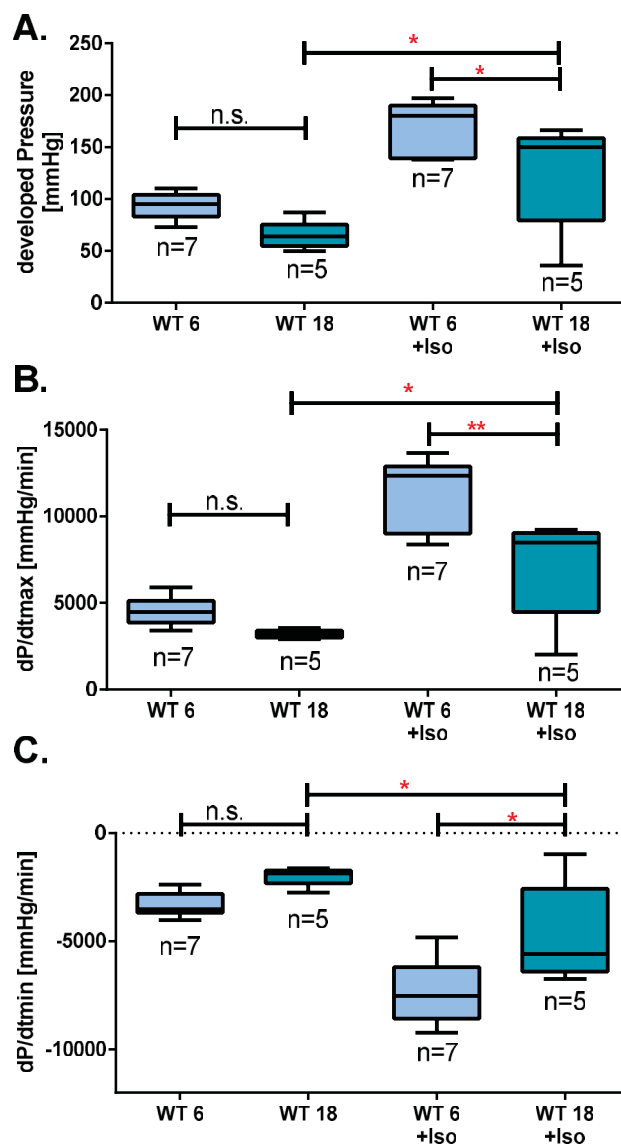


Figure 29: Cardiac function of young and old WT mice

Baseline DP (A.), dP/dtmax (B.) and dP/dtmin (C.) were not different between 6 months old and 18 months old WT mice. After stimulation with isoproterenol 18 months old WT hearts responded with a significant increase in DP, dP/dtmax and dP/dtmin. Response to isoproterenol was significantly lower in 18 months old WT mice compared to 6 months old WT mice. (n.s. not significant; *p<0.05; **p<0.01; ***p<0.0001; 1-way ANOVA, Bonferroni post-hoc)

There were no differences between 18 months old and 6 months old hearts under baseline conditions. After stimulation with Iso all hearts responded with an increase of DP, dP/dtmax and dP/dtmin. Inotropic (DP, dP/dtmax) and lusitropic (dP/dtmin) response of 18 months old WT hearts was significant lower compared to 6 months old WT hearts, whereas response of 18 months old Nrf2 KO hearts was not different.

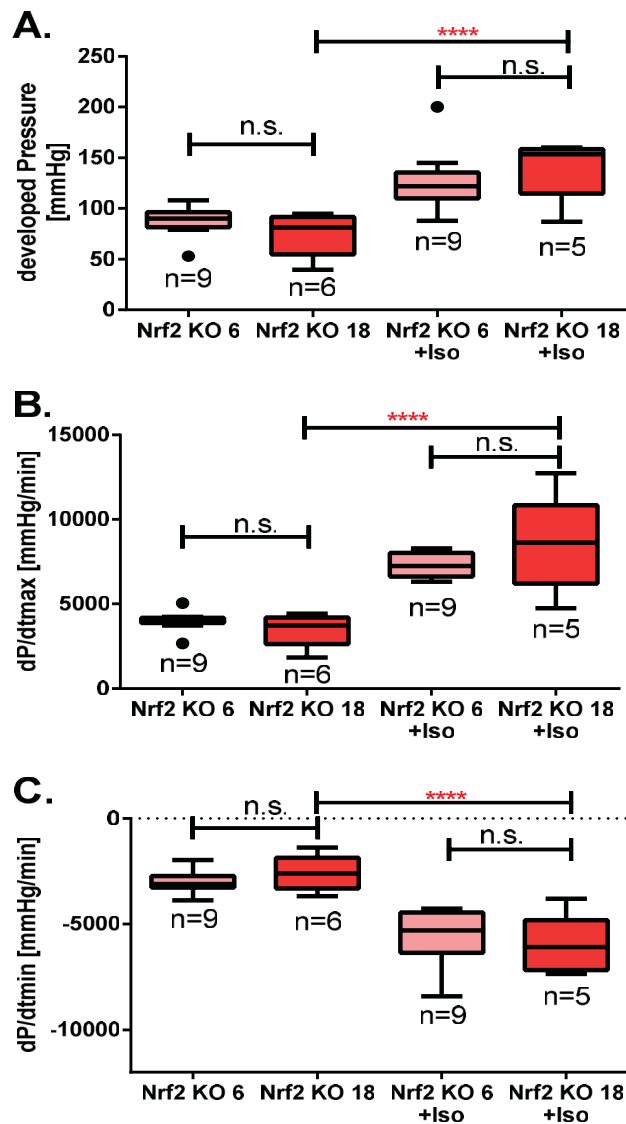


Figure 30 Cardiac function of young and old Nrf2 KO mice

Baseline DP (A.), dP/dtmax (B.) and dP/dtmin (C.) were not significantly different between 6 months old and 18 months old Nrf2 KO mice. Stimulation with isoproterenol resulted in a significant increase in DP, dP/dtmax and dP/dtmin. Response to isoproterenol was not significantly different between 6 month old and 18 months old Nrf2 KO hearts. (n.s. not significant, ****p<0.0001, 1-way ANOVA, Bonferroni post-hoc)

Comparing isolated hearts of 18 months old WT and Nrf2 KO mice there were no differences in baseline DP, dP/dtmax and dP/dtmin (Figure 31).

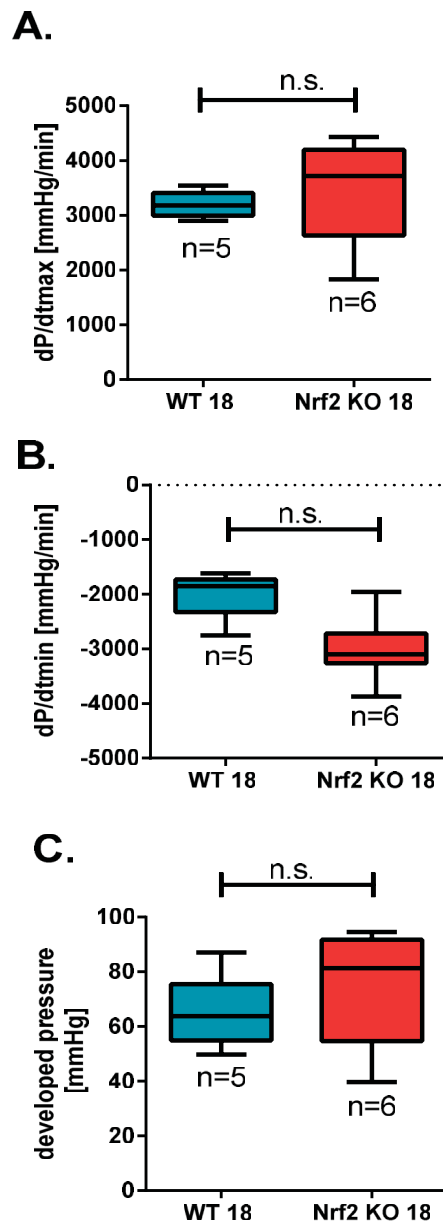


Figure 31: Contractility of 18 months old Nrf2 KO and WT mice

Hearts of 18 months old Nrf2 KO mice showed no significant differences in DP (A.), dP/dtmax (B.) and dP/dtmin (C.) compared to 18 months old WT mice. (unpaired t-test, n.s. not significant)

Inotropic (dP/dtmax, DP) and lusitropic (dP/dtmin) response to isoproterenol of 18 months old Nrf2 KO hearts is not different to 18 months old WT hearts, whereas there is a difference in the age of 6 months (Figure 28, Figure 30).

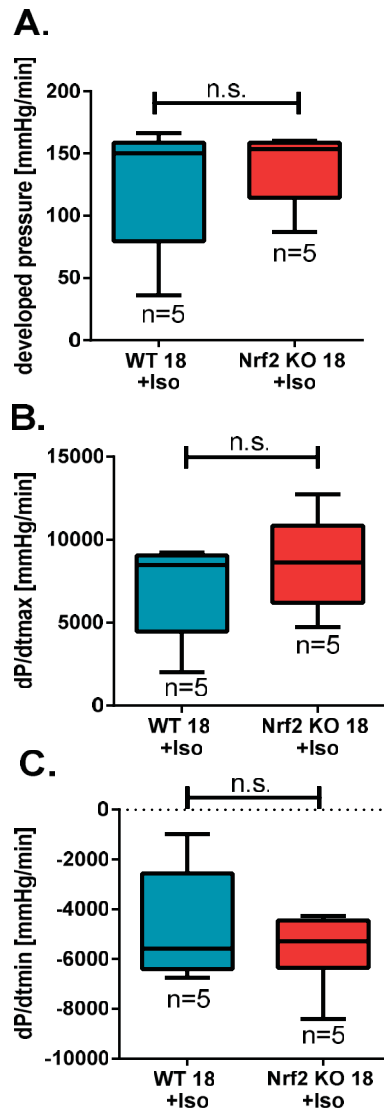


Figure 32: Contractility of old hearts after stimulation with Iso

dP/dtmax (A.) and dp/dtmin (B.) was significantly different between hearts of 6 months old Nrf2 KO (Nrf2 KO 6) and WT (WT 6) mice after stimulation with isoproterenol (+Iso). Hearts of 18 months old Nrf2 KO (Nrf2 KO 18) and WT (WT18) mice showed no differences in dP/dtmax or dP/dtmin. (1-way ANOVA, Bonferroni post-hoc, n.s. not significant, *p<0.05, **p<0.01)

5.3. Coronary function of Nrf2 KO mice

To analyze coronary function of 6 months old Nrf2 KO mice coronary flow of isolated hearts was assessed and increase of flow after short time ischemia (reactive hyperemia) was analyzed. There was no significant difference in baseline coronary flow and reactive hyperemic response compared to WT mice (Table 13).

coronary flow	WT 6 months old n=7	Nrf2 KO 6 months old n=9
baseline (ml/min)	3.44 (± 0.55)	3.66 (± 1)
reactive hyperemia (ml/min)	8.35 (± 0.67)	8.89 (± 1.45)

Table 13: Baseline coronary flow
(unpaired t-test, not significant)

After administration of endothelium dependent bradykinin and adenosine, coronary flow increased in hearts of Nrf2 KO and WT littermates. There was no significant difference between both groups (Figure 33). Increased coronary flow implicated increased contractility. There were no differences in increase of DP, dP/dtmax or dp/dtmin (data not shown).

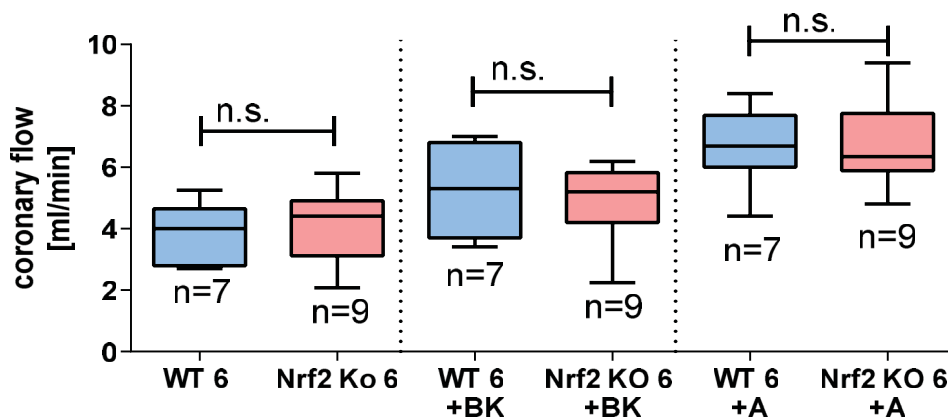


Figure 33: Coronary flow baseline and after drug treatment

Nrf2 KO and WT mice did not show significant differences in baseline coronary flow, nor coronary dilation after bradykinin (+BK), nor adenosine (+A) administration. (n.s. not significant; 1-way ANOVA, Bonferroni post-hoc, $p < 0.05$)

To investigate whether aging affects coronary flow of Nrf2 KO mice and WT mice, isolated hearts of 18 months old Nrf2 KO and WT mice were analyzed. Baseline coronary flow, increase of flow after short time ischemia and after administration of bradykinin and adenosine was measured. Baseline coronary flow and reactive hyperemia were not different in hearts of 18 months old Nrf2 KO and WT mice compared to their 6 months old littermates (Figure 34).

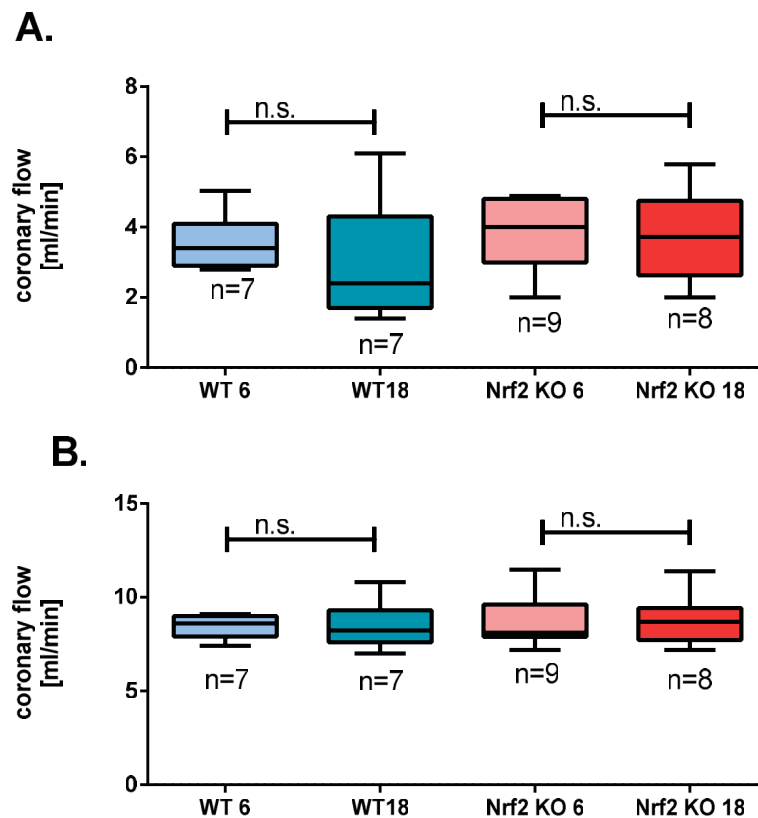


Figure 34: Coronary flow of young and old mice

There were no differences in baseline flow (A.) and reactive hyperemia (B.) of 18 months old WT and Nrf2 KO hearts compared to 6 old littermates. (1-way ANOVA, Bonferroni post-hoc)

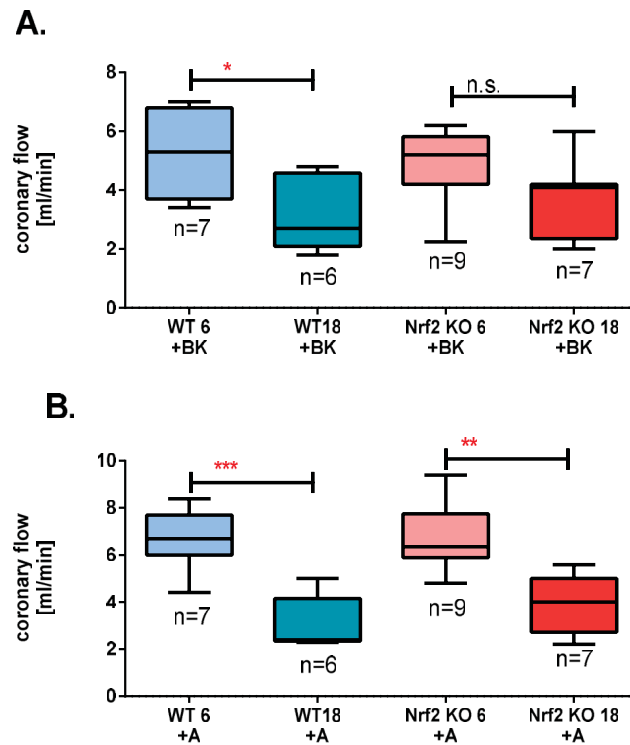


Figure 35: Coronary flow of young and old mice

(A.) Response to bradykinin (+BK) was significantly decreased in isolated hearts of 18 months old WT mice compared to 6 months old WT mice. Response to bradykinin of isolated hearts of 18 months old Nrf2 KO mice was not different to 6 months old Nrf2 KO mice. (B.) Coronary vasodilation after stimulation with adenosine (+A) was lower in isolated hearts of 18 months old Nrf2 KO and WT mice compared to their 6 months old littermates.

(n.s. not significant; * $p < 0.05$, ** $p < 0.01$, *** $p < 0.001$; 1-way ANOVA, Bonferroni post-hoc)

Increase of coronary flow after administration of bradykinin (Figure 35) was significantly lower in hearts of 18 months old WT mice, whereas 18 months old Nrf2 KO mice showed no differences in increase of flow compared to their younger littermates. After administration of adenosine (Figure 35), hearts of 18 month old Nrf2 KO and WT mice responded with a significantly lower increase of coronary flow compared to their 6 months old littermates.

6. Discussion

The aim of this study was to characterize cardiovascular function of young and old Nrf2 KO mice (Figure 36).

Nrf2 KO mice show dysregulated cardiac function as determined by decreased diastolic function (prolonged DT, MVET, IVRT, increased E/A ratio and MPI), lower response to inotropic stimulation in vivo (PES, dP/dtmax, dP/dtmin) and in isolated perfused hearts (DP, dP/dtmax, dP/dtmin). Coronary function of Nrf2 KO mice is preserved as determined by unaltered coronary dilation (Flow). Preserved coronary and dysregulated left ventricular function is accompanied by significant hypotension in Nrf2 KO mice.

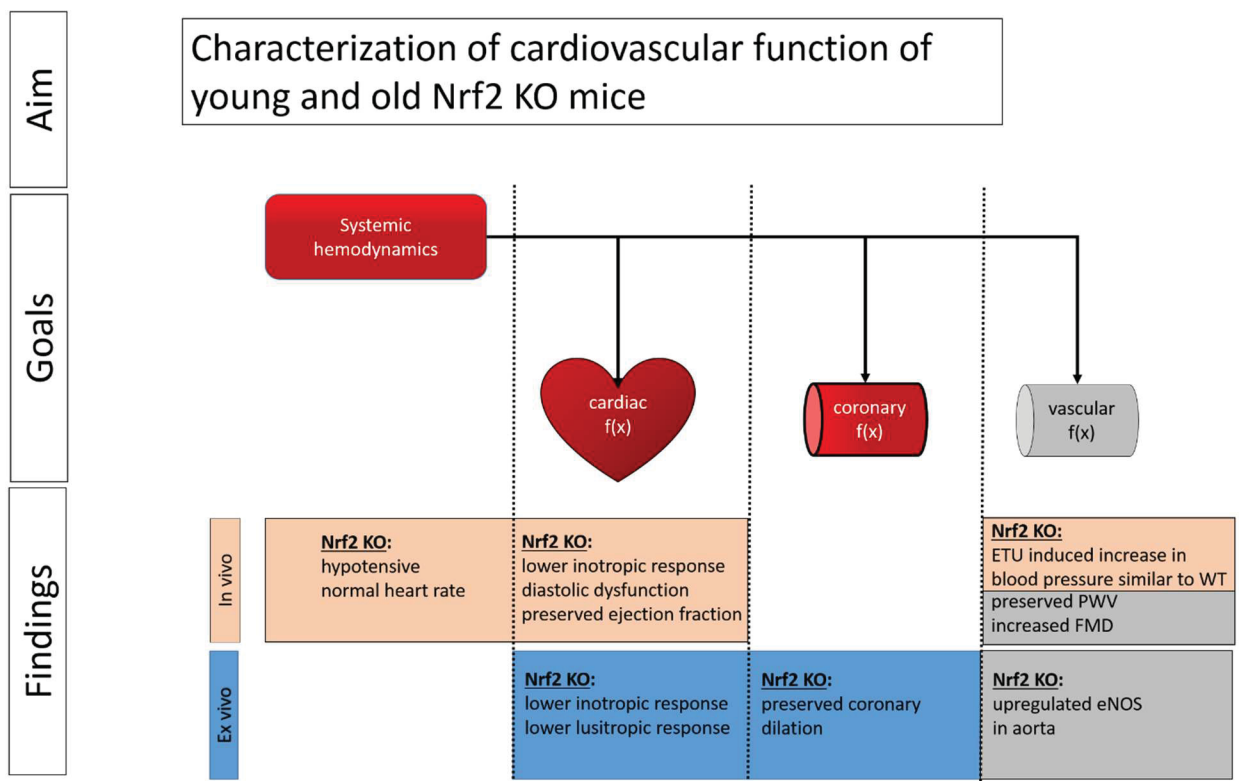


Figure 36: Outline

The results show how the absence of Nrf2 affects hemodynamics, cardiac function, coronary function and peripheral vascular function of mice. Grey colored findings were investigated by others and are discussed in context.

6.1. Nrf2 KO mice show lower blood pressure with unchanged heart rate

Nrf2 KO mice show a significant decreased MAP as compared to WT littermates without differences in HR. This hypotension is not influenced by age.

There are just few other studies which analyzed blood pressure in Nrf2 KO mice. Li et al. [72, 73] investigated the role of Nrf2 in cardiac remodeling. They also measured blood pressure in Nrf2 KO mice and WT mice as positive control. In contrast to the here presented results, they could not show significant differences in baseline blood pressure. There are several methodical differences (strain, age, method of blood pressure assessment) between the studies of Li et al. and this work.

For both studies Li et al. used 8 weeks old Nrf2 deficient mice with a SV129 background and compared them to WT SV129 mice. In this work we used 6 months old and 18 months old Nrf2 KO mice with a C57bl/6 background and compared them to WT C57bl/6 mice. There are several differences known between SV129 and C57bl/6 mice. SV129 backgrounded Nrf2 KO mice show an inflammatory state and develop autoimmune like diseases [72, 118]. It was proved whether the here presented Nrf2 KO mice on C57bl/6 background are also prone to inflammation and C57bl/6 Nrf2 KO mice do not show any signs of proinflammatory state [1]. Cardiovascular pathologies are often associated to inflammation. Therefore, the genetically differences of C57bl/6 and SV129 mice and the proinflammatory state of SV129 Nrf2 KO mice may explain the different results of this work and the study of Li et al.

A second bias might be the methodical differences in blood pressure measurement. Li et al. used two different techniques: Tail cuff method and bilateral invasive measurements. The tail cuff system measures peripheral arterial pressure. This does not reflect central arterial pressure because the tail artery is very sensitive to environmental temperature, blood volume status and vascular tone [119]. In the here presented work central arterial pressure was directly measured by invasive pressure-volume catheterization (Millar) of the ascending aorta and environmental settings were continuously controlled. When Li et al. measured with Millar catheter they did a bilateral occlusion of

carotid arteries. Although arterial perfusion of the brain is more variable in mice than in human [120] it has been shown that bilateral ligation of the carotid arteries influences blood pressure and that this influence differs from C57bl/6 to SV129 [121]. In the here presented work only the right carotid artery was occluded while perfusion of other vessels was not directly diminished.

To evaluate if systemic hemodynamics of Nrf2 KO mice differ with increasing age, 18 months old mice were assessed. 18 months old Nrf2 KO mice showed neither significant differences in blood pressure nor in HR compared to 6 months old Nrf2 KO mice. Therefore, it can be concluded that lower blood pressure of Nrf2 KO mice is permanent and not age dependent which is similar to WT mice. Different from humans aging in WT mice is not associated with elevated blood pressure [122, 123]. The results confirm that blood pressure in WT mice is unaffected of increased age. This is consistent with other studies which could not find any changes in systolic, diastolic or mean arterial pressure in WT C57bl/6 mice [122, 123].

Here, evidence was presented that deficiency of Nrf2 affects systemic hemodynamics of mice. Young and old Nrf2 KO mice are significantly hypotensive compared to WT mice, while heart rate is unaffected. These changes in blood pressure could be based on differences in cardiac or vascular function which are discussed below.

6.2. Left-ventricular function is dysregulated in Nrf2 KO mice

The presented changes in systemic hemodynamics may be dependent on differences in cardiac function.

Echocardiographic assessment showed diastolic dysfunction with preserved ejection fraction in Nrf2 KO mice. In vivo Nrf2 KO mice showed lower response to beta-adrenergic and cardiac glycoside treatment. Lower inotropic and lusitropic response could be also confirmed ex vivo in isolated hearts. Further, aging does not aggravate the impaired cardiac function of Nrf2 KO mice. Cardiac dysfunction of Nrf2 KO mice is also coupled to structural defects

shown in increased LV hypertrophy as determined by increased LV mass to body weight ratio.

Stimulation of cardiac beta receptors leads to positive inotropic, positive chronotropic, positive lusitropic, positive dromotropic and positive bathmotropic response. Nrf2 KO mice showed lower inotropic increase (dp, dP/dtmax) and lower lusitropic increase (dP/dtmin), whereas chronotropic, dromotropic and bathmotropic response was not effected (HR). Therefore lower response to beta-adrenergic stimulation is not based on lower density of beta receptors but reveals a downstream problem of cardiac function. If Nrf2 KO mice would have lower density of beta receptors, one would expect a lower response in all beta-adrenergic effects. Anyway, there were no differences neither in chronotropic, nor in dromotropic, nor in bathmotropic response. Besides, Nrf2 KO also diminishes Ouabain response and Nrf2 KO mice show dysregulated diastolic function.

Response to beta agonists, response to ouabain and diastolic function are all dependent on intracellular Ca^{2+} concentration. Thus it is likely that Nrf2 KO mice have problems in Ca^{2+} handling.

Degraded lusitropy and diastolic dysfunction in Nrf2 KO mice is consistent with data showing that (ionizing radiation induced) oxidative stress caused diastolic Ca^{2+} overload in cardiac myocytes [124]. Sag et al. could show that increased oxidative stress resulted in slower relaxation kinetics. This work is the first which showed that lack of Nrf2 results in slower relaxation kinetics and lower lusitropic responsiveness.

The diastolic Ca^{2+} shift from cytoplasm into SR by SERCA is known to be regulated by oxidation/reduction of SERCA protein [67, 125]. It has been shown that increase of intracellular ROS or/and increase of mitochondrial ROS production are able to decrease SERCA activity [67]. SERCA2a is the predominant isoform in cardiac tissue and the best studied isoform in regard to diastolic dysfunction [126-128]. In further experiments it was shown that SERCA2a is downregulated in myocardium of Nrf2 KO mice [1]. If expression of SERCA2a is downregulated in cardiac cells of Nrf2 KO mice, Ca^{2+}

sequestration into sarcoplasm is prolonged in those mice. This is aggravated when the amount of cytosolic Ca^{2+} is higher through stimulation with Ouabain which blocks $\text{Na}^+/\text{Ca}^{2+}$ exchanger and thereby amplifies the demand for SERCA.

In isolated hearts of Nrf2 KO mice relaxation is also dysregulated. Although we can detect a normal relaxation of isolated Nrf2 KO hearts in baseline settings, isolated hearts of Nrf2 KO mice show decreased responsiveness to beta agonists. SERCA2a downregulation might be also responsible for the reduced $\text{dP/dt}_{\text{min}}$ after stimulation with beta agonists. Lusitropic response to beta stimulation is mediated by inactivation of SERCA inhibition. Stimulation of beta receptors inactivates phospholamban (PLB) the physiological inhibitor of SERCA. Lower expression of SERCA2a in Nrf2 KO mice might be accompanied by less reserve for augmentation of functional SERCA.

PLB is regulated by phosphorylation (e.g. PKA) and the Ca^{2+} concentration itself [126]. Taking into regard that oxidative stress causes diastolic Ca^{2+} overload [124], it could be speculated that lack of Nrf2 is accompanied by increased Ca^{2+} concentration. Increased intracellular Ca^{2+} concentration inactivates PLB. As a result there will be less PLB disposed for PKA phosphorylation and consequently lower lusitropic response after beta stimulation. However, we can only speculate about PLB in Nrf2 KO mice and further studies have to point out whether PLB is dysregulated in Nrf2 KO mice or not.

There was a difference between diastolic function of isolated hearts of old WT and Nrf2 KO mice. In both groups baseline $\text{dP/dt}_{\text{min}}$ was not different to young littermates. Stimulation with isoproterenol showed significant reduced $\text{dP/dt}_{\text{min}}$ in hearts of old WT mice compared to their younger littermates. In old Nrf2 KO mice $\text{dP/dt}_{\text{min}}$ response to isoproterenol was not different to young age. Reduced lusitropic response to beta mimetics in aged hearts of WT mice is consistent with other studies showing impaired diastolic function in aged WT hearts [56, 85, 129-136]. SERCA activity and expression are influenced by aging [56, 131-136] which is at least partial due to decreased antioxidative capacity [134, 135]. Lack of antioxidant capacity in young Nrf2 KO mice is associated to diastolic dysfunction which is not aggravating with increase of age. Therefore, age dependent impairment of diastolic function

seems to be prematurely in Nrf2 KO mice. Therefore Nrf2 KO mice may represent a model for further investigations of diastolic dysfunction.

Summarized, global lack of Nrf2 results in SERCA2a downregulation causing impaired cardiac relaxation and degraded lusitropy, which is independent of age. However, lusitropy of WT mice declines with age. SERCA2a downregulation is probably responsible for diastolic dysfunction and impaired lusitropic response of Nrf2 KO mice.

Systolic function was preserved in echocardiographic measurements of Nrf2 KO mice and baseline contractility of isolated hearts was not different to WT mice. Miller catheter assessment showed that baseline PES was lower in Nrf2 KO mice which is associated with the above shown lower blood pressure. Nevertheless cardiac contractility is affected by lack of Nrf2 shown in decreased inotropic responsiveness to ouabain and beta-agonists.

Lower response of Nrf2 KO mice to beta-adrenergic stimulation is in agreement with data obtained by Kubin et al. [137]. In isolated perfused hearts with normal left ventricular function they have shown that beta adrenergic response to dobutamin could be augmented by increasing antioxidant capacity, suggesting a negative effect of endogenous ROS to inotropic response [137].

There are no other studies focusing on Nrf2 deficiency and cardiac inotropic state, thus we can only speculate about the changes in inotropic state of Nrf2 KO mice, but several studies have examined the impact of oxidative stress to PKA pathway [26, 138] and its inotropic targets: cardiac L-type Ca^{2+} channels [67, 139-141], RyR [67, 125] and the contractile filaments [26, 142]. Several oxidative modifications of PKA protein have been detected which enhance contractility of cardiac cells with increased oxidative stress independent of beta adrenergic stimulation [138]. This might contribute to preservation of baseline contractile function of Nrf2 KO mice and hereby reduce possible augmentation of PKA activity through adrenergic stimulation.

Similar to diastolic function hearts of 18 months old Nrf2 KO mice did not show any significant differences in DP and dP/dtmax compared to young Nrf2 KO

mice. Baseline DP and dP/dtmax of isolated hearts of old WT mice was not different to 6 months old isolated hearts, but 18 months old WT hearts showed lower inotropic response (DP, dP/dtmax) after stimulation with beta agonists compared to young.

Lower contractility of old WT hearts is consistent with other studies showing that cardiac Ca²⁺ handling gets attenuated by aging [143]. This decrease of cardiac contractility is at least partial due to increased oxidative damage of proteins involved in cardiac Ca²⁺ handling [15, 136]. Jiang et al. have also shown that inotropic response to Iso is lower in hearts of aged rats [129].

Further, preserved baseline contractility of aged Nrf2 KO and WT mice might contribute to the above shown independency of blood pressure from age.

6.3. Coronary function is preserved in Nrf2 KO mice

Coronary arteries of 6 months old Nrf2 KO mice showed no significant differences to WT mice in basal flow, reactive hyperemic response and vasodilation after administration of bradykinin or adenosine. Coronary arteries of 18 months old WT mice dilate less after administration of adenosine and bradykinin compared to their younger littermates. In contrast, coronary arteries of 18 months old Nrf2 KO mice respond with a lower response to adenosine but with no differences in bradykinin response compared to 6 months old Nrf2 KO mice. Besides these findings in coronary function, blood pressure increased to the same amount after administration of eNOS inhibitor ETU in 6 months old Nrf2 KO and WT mice.

The here reported results have to be discussed in context with other experiments performed by other member of the laboratory which have assessed vascular function of Nrf2 KO mice. These experiments have been published together with parts of this thesis as one study [1]. In that study evidence was presented that vascular function of Nrf2 KO mice is preserved. The team has shown that eNOS levels in aorta of Nrf2 KO mice are twofold higher than in WT mice, that eNOS stimulation of aortic rings of Nrf2 KO mice resulted in a significant higher cGMP concentration and that in vivo vascular

function is preserved. In vivo, Nrf2 KO mice have preserved pulse wave velocity (pwv) and increased maximal dilation after vascular occlusion of femoral artery compared to WT mice, which is known as eNOS dependent flow mediated dilation (FMD) [1].

Other studies have also shown that aortic rings of Nrf2 KO mice have preserved relaxation and constriction [5]. Thus we can conclude Nrf2 KO mice have fully preserved vascular and coronary function.

Moreover, there were differences in coronary function of aged mice. Aging in WT mice is accompanied by restriction in coronary function -endothelium dependent and independent. This is consistent with other studies which have shown that aging is connected to changes in flow mediated dilation [123, 144] and vascular stiffness [122, 123].

Coronary response to adenosine of old Nrf2 KO mice is also decreased, but response to endothelium dependent bradykinin is not different as compared to young Nrf2 KO mice. As eNOS dependent bradykinin response is not decreasing with aging in Nrf2 KO mice, but decreases in WT mice it can be assumed that upregulation of eNOS may also be present in coronary arteries of Nrf2 KO mice and that upregulation of eNOS is not limited to young but keeps on to maturity.

Others have also reported a linking between Nrf2 and NO dependent vasorelaxation [145]. Whereas, Heiss et al. reported an increase of NO bioavailability after Nrf2 stimulation in endothelial cells [146]. This could be seen in contrast to the here presented study. However, the experiments of Heiss et al. were obtained in cell culture and the results have to be interpreted with caution as transfer to living animals is limited. Another source of uncertainty is that Heiss et al. could show decreased eNOS expression after Nrf2 stimulation. Consequently, one would expect uncoupled eNOS in Nrf2 KO mice. In contrast the here presented study could show that deficiency of Nrf2 increases eNOS expression in vitro. Functionality of increased eNOS in Nrf2 KO mice was confirmed by preserved coronary function (isolated hearts) and vascular function (aortic rings, pwv, FMD, Millar). Therefore, this study can not

reach that eNOS is uncoupled in Nrf2 KO mice. Rather, deficiency of Nrf2 seems to have a positive effect on eNOS dependent vascular function.

Increase of ROS and oxidative stress could be a possible mediator for eNOS regulation in Nrf2 KO mice. Previous studies have evaluated that increase of H₂O₂ stimulates eNOS expression and stabilizes eNOS message [147-149] but we are still lacking of a concrete biochemical linking between Nrf2 and eNOS. Further research is required to explore how lack of Nrf2 increases eNOS expression.

To summarize, coronary function is preserved in Nrf2 KO mice and knock out of Nrf2 leads to elevated levels of eNOS which may contribute to hypotension.

6.4. Conclusion and outlook

Taken together the results confirm the hypothesis that Nrf2 deficiency affects cardiovascular phenotype. This work presents a comprehensive characterization of cardiovascular function of Nrf2 KO mice and provided evidence how knock out of Nrf2 influences hemodynamics, cardiac function, coronary function and peripheral vascular function.

Nrf2 KO mice show lower blood pressure by unaltered heart rate which is based on an interplay between changes in left-ventricular and vascular function. Coronary function of Nrf2 KO mice is preserved. Cardiac function of Nrf2 KO mice is characterized by diastolic dysfunction, lower inotropic and lusitropic responsiveness, which is probably based on problems in cardiac Ca²⁺ handling, shown in SERCA2a downregulation. Dysregulated cardiac function is linked to cardiac hypertrophy in Nrf2 KO mice. Nrf2 KO mice have preserved peripheral vascular and coronary function with overexpression of eNOS and show increased flow mediated dilation in the femoral artery.

Aging did not change baseline cardiovascular function of WT and Nrf2 KO mice. Nevertheless, inotropic and lusitropic response of hearts of Nrf2 KO mice did not show an age dependent decrease, which was shown in WT mice. Coronary response to bradykinin and adenosine was also decrease in old WT mice. Whereas in old Nrf2 KO mice only response to adenosine was decreased compared to young Nrf2 KO mice.

Despite all elucidated interactions of Nrf2 and cardiac and coronary function, this study was the first which investigated hemodynamics of Nrf2 KO mice. Most of the studies which use Nrf2 KO mice chose mice with SV129 background. This might be an important bias because cardiovascular pathologies are often accompanied by inflammation and SV129 backgrounded Nrf2 KO mice show an inflammatory state and develop autoimmune like diseases [72, 118]. Evidence has been given that Nrf2 KO mice with C57bl/6 background do not show a proinflammatory state [1] but further studies have to confirm whether the here presented results are transferable to Nrf2 KO mice with another genetically background.

For the first time we linked cardiovascular function with decreased antioxidant defense in vivo and isolated hearts. However, more research is required to develop a full picture of the cardiovascular pathways influenced by lack of Nrf2. eNOS upregulation was determined as an important difference in vascular function. SERCA2a downregulation was determined as an important difference in diastolic function of Nrf2 KO mice. Additionally, lower inotropic responsiveness of Nrf2 KO mice might also represent a dysregulation in other cellular pathways which should be elucidated in further studies. In this context, the literature gives us suggestions for future investigations on Nrf2 KO mice and inotropic response. The central player for inotropic response is the PKA pathway, that has already been focused by several studies, which have examined the impact of oxidative stress to PKA pathway [26, 138] and its inotropic targets [150]: cardiac L-type Ca^{2+} channels [67, 139-141], RyR [67, 125] and the contractile filaments [26, 142]. Assessment of the influence of ROS to L-type Ca^{2+} channels have revealed partial contradictory results. Elevation of cytoplasmic ROS levels are suggested to enhance open probability of L-type channels via S-glutathionylation [140]. Ca^{2+} current is lower in cardiac myocytes of patients with atrial fibrillation and it has been shown that lower Ca^{2+} current is due to enhanced S-nitrosylation of L-type Ca^{2+} channels caused by decreased levels of GSH in those patients [141]. Redox modification of RyR is less controversial. Opposite to SERCA, activity and expression of RyR is upregulated by increase of oxidative stress [67, 125]. If deficiency of Nrf2 alters RyR expression or activity is still unclear. ROS also influence the

contractile units by interacting with several kinases and phosphatases. The literature provides several in part controversial effects of ROS and ROS-activated enzymes on the myofilament lattice [26]. Most studies were undertaken in vitro focusing on single filaments and it is still unclear how these numerous effects interplay in vivo, so Nrf2 KO mice may present a model for in vivo investigation on that.

Summarized, in this work presented influence of Nrf2 and decreased antioxidative defense on cardiovascular function gives us new considerations for future investigations. Solving these questions may solidify our understanding of antioxidant capacity in cardiovascular health and diseases, which may give us new approach for medical strategies. Furthermore, lack of antioxidative capacity seems to play a major role in the pathology of diastolic dysfunction, a common, but incomplete understood disease [151]. The crosstalk between Nrf2 and SERCA2a might be potential pharmacological target and further studies are needed to get a deeper understanding of this interaction.

List of abbreviations

·OH	hydroxy radical
A1-, A2A-, A2B-, A3-AR	Adenosin receptors
Ach	acetylcholine
ANS	autonomic nerve system
ARE	antioxidant response element
AV	aortic valve
BK1-, BK2-R	bradykinin receptor
bpm	beats per minute
bZIP	basic leucine zipper domain
Ca ²⁺	calcium
CaM	Ca ²⁺ /Calmodulin complex
cAMP	cyclic adenosine monophosphate
cGMP	cyclic guanosine monophosphate
CO	cardiac output
Cul3	Cullin 3
cVSMC	coronary vasscular smooth muscle cell
CYP	cytochrom P450 oxydase
cys	cystein
DNA	deoxyribonucleic acid
DP	developed pressure
dP/dtmax	maximum of rate of left ventricular pressure rise
dP/dtmin	minimum of rate of left ventricular pressure decrease
DT	E wave deceleration time
EDHF	endothelium derived hyperpolarizing factor
EDV	end diastolic volume
EF	ejection fraction
eNOS	endothelial NO synthase
ESV	end systolic volume
ETU	2-ethyl-2-thiopseudourea
Fe ²⁺	iron
Flow	coronary flow

FS	fractional shortening
FTH	ferritin heavy chain
FTL	ferritin light chain
G6PD	glucose-6-phosphate dehydrogenase
GCL	glutamate-cysteine ligase
GIT	gastrointestinal tract
GPX	glutathione peroxidase
GSH	glutathione (reduced form)
GSR	glutathione reductase
GSSG	glutathione (oxidized form)
GSTA	glutathione S-transferase
H ₂ O ₂	hydrogenperoxid
hemostat	hemostatic clamp
HO-1	haem oxygenase 1
HR	heart rate
I	current
i.p.	intraperitoneal injection
IDH1	isocitrate dehydrogenase
iNOS	inducible NO synthase
IVC	isovolumetric contraction
IVCT	isovolumetric contraction time
IVR	isovolumetric relaxation
IVRT	isovolumetric relaxation time
K ⁺	potassium
Keap1	Kelch like ECH-associated protein 1
Langendorff	isolated perfused heart model
LV	left ventricle
MAP	mean atrial pressure
ME1	malic enzyme 1
MHC	myosin heavy chain
Millar	pressure-volume catheter
MLCK	myosin light chain kinase
MLCP	myosin light chain phosphatase

MPI	myocardial performance index
MV	mitral valve
MVET	mitral valve ejection time
Na ⁺	sodium
NADPH	nicotinamide-adenine-dinucleotid-phosphate
NCX	sodium/calcium antiporter
NF-E2	Nuclear Factor Erythroid 2
nNOS	neural NO synthase
NO	nitric oxid
NOS	NO synthase
Nox	NADPH oxidase
NQO	NADPH:quinone oxidoreductase
Nrf2	nuclear factor erythroid 2 related factor 2
Nrf2 KO	Nrf2 Knock out
O ₂	oxygen
O ₂ ⁻	superoxide radical
Pdia	diastolic pressure
PED	end diasystolic pressure
PES	end systolic pressure
PHGDH	phosphoglycerate dehydrogenase
PKA	protein kinase A
PKC	protein kinase C
PKG	protein kinase G
PLB	phospholamban
PLC	phospholipase C
Pmean	mean arterial pressure
Psys	systolic pressure
Pxn	peroxiredoxin
RCCA	right common carotid artery
RNA	ribonucleic acid
RNS	reactive nitrogen species
ROS	reactive oxygen species
RVU	relative volume unit

RyR	ryanodin receptor		
SERCA	sarcoplasmic/endoplasmic ATPase	reticulum	Ca ²⁺
SOD	superoxid dismutase		
SR	sarcoplasmic reticulum		
SV	stroke volume		
SVR	systemic vascular resistance		
Txn	Thioredoxin		
TXNRD	thioredoxin reductase		
VSMC	vascular smooth muscle cell		
WT	wild type		
XCT	cystine/glutamate transporter		

References

1. Erkens, R., et al., *Left ventricular diastolic dysfunction in Nrf2 knock out mice is associated with cardiac hypertrophy, decreased expression of SERCA2a, and preserved endothelial function*. Free Radic Biol Med, 2015. **89**: p. 906-17.
2. Statistisches Bundesamt, *Krankheitskosten Fachserie 12, Reihe 7.2, 2002-2008*. 2010: Wiesbaden.
3. Ezzati, M., et al., *Contributions of risk factors and medical care to cardiovascular mortality trends*. Nat Rev Cardiol, 2015. **12**(9): p. 508-530.
4. Sies, H., *Oxidative stress: a concept in redox biology and medicine*. Redox Biol, 2015. **4**: p. 180-3.
5. Ding, Y., et al., *Dietary ellagic acid improves oxidant-induced endothelial dysfunction and atherosclerosis: role of Nrf2 activation*. Int J Cardiol, 2014. **175**(3): p. 508-14.
6. Kojda, G. and D. Harrison, *Interactions between NO and reactive oxygen species: pathophysiological importance in atherosclerosis, hypertension, diabetes and heart failure*. Cardiovasc Res, 1999. **43**(3): p. 562-71.
7. Wang, J.C. and M. Bennett, *Aging and atherosclerosis: mechanisms, functional consequences, and potential therapeutics for cellular senescence*. Circ Res, 2012. **111**(2): p. 245-59.
8. Fanelli, C. and R. Zatz, *Linking oxidative stress, the renin-angiotensin system, and hypertension*. Hypertension, 2011. **57**(3): p. 373-4.
9. Touyz, R.M. and E.L. Schiffrin, *Reactive oxygen species in vascular biology: implications in hypertension*. Histochem Cell Biol, 2004. **122**(4): p. 339-52.
10. Howden, R., *Nrf2 and cardiovascular defense*. Oxid Med Cell Longev, 2013. **2013**: p. 104308.
11. Ceconi, C., et al., *Oxidative stress in cardiovascular disease: myth or fact?* Archives of Biochemistry and Biophysics, 2003. **420**(2): p. 217-221.
12. De Hert, S., *Physiology of hemodynamic homeostasis*. Best Pract Res Clin Anaesthesiol, 2012. **26**(4): p. 409-19.
13. Bruno, R.M., et al., *Sympathetic regulation of vascular function in health and disease*. Front Physiol, 2012. **3**: p. 284.
14. Klinker R., et al., *Physiologie*. 6. ed. 2009: Thieme Verlag.
15. Cooper, L.L., et al., *Redox modification of ryanodine receptors by mitochondria-derived reactive oxygen species contributes to aberrant Ca²⁺ handling in ageing rabbit hearts*. J Physiol, 2013. **591**(Pt 23): p. 5895-911.
16. Weisleder, N. and J. Ma, *Altered Ca²⁺ sparks in aging skeletal and cardiac muscle*. Ageing Res Rev, 2008. **7**(3): p. 177-88.
17. Feigl, E.O., *Berne's adenosine hypothesis of coronary blood flow control*. American Journal of Physiology - Heart and Circulatory Physiology, 2004. **287**(5): p. H1891-H1894.
18. Layland, J., et al., *Adenosine: physiology, pharmacology, and clinical applications*. JACC Cardiovasc Interv, 2014. **7**(6): p. 581-91.
19. Gan, L.M., J. Wikstrom, and R. Fritsche-Danielson, *Coronary flow reserve from mouse to man--from mechanistic understanding to future interventions*. J Cardiovasc Transl Res, 2013. **6**(5): p. 715-28.
20. Gould, K.L., et al., *Anatomic versus physiologic assessment of coronary artery disease. Role of coronary flow reserve, fractional flow reserve, and positron emission tomography imaging in revascularization decision-making*. J Am Coll Cardiol, 2013. **62**(18): p. 1639-53.

21. Meimoun, P. and C. Tribouilloy, *Non-invasive assessment of coronary flow and coronary flow reserve by transthoracic Doppler echocardiography: a magic tool for the real world.* Eur J Echocardiogr, 2008. **9**(4): p. 449-57.
22. Rigo, F., *Coronary flow reserve in stress-echo lab. From pathophysiologic toy to diagnostic tool.* Cardiovasc Ultrasound, 2005. **3**: p. 8.
23. Higashi, Y., *Assessment of endothelial function. History, methodological aspects, and clinical perspectives.* Int Heart J, 2015. **56**(2): p. 125-34.
24. Treasure, C.B., et al., *Hypertension and left ventricular hypertrophy are associated with impaired endothelium-mediated relaxation in human coronary resistance vessels.* Circulation, 1993. **87**(1): p. 86-93.
25. Valko, M., et al., *Free radicals, metals and antioxidants in oxidative stress-induced cancer.* Chemico-Biological Interactions, 2006. **160**(1): p. 1-40.
26. Steinberg, S.F., *Oxidative stress and sarcomeric proteins.* Circ Res, 2013. **112**(2): p. 393-405.
27. Stadtman, E.R., *Protein oxidation in aging and age-related diseases.* Ann N Y Acad Sci, 2001. **928**: p. 22-38.
28. Levine, R.L. and E.R. Stadtman, *Oxidative modification of proteins during aging.* Exp Gerontol, 2001. **36**(9): p. 1495-502.
29. Stadtman, E.R., *Protein oxidation and aging.* Free Radic Res, 2006. **40**(12): p. 1250-8.
30. Rohrig, R., *Wirkung von Flavonoiden auf den redoxsensitiven Nrf2-Signalweg in Säugerzellen, Inaugural-Dissertation, in Math.-Nat. Fakultät.* 2010, Heinrich-Heine-Universität Düsseldorf.
31. Dizdaroglu, M., et al., *Free radical-induced damage to DNA: mechanisms and measurement.* Free Radic Biol Med, 2002. **32**(11): p. 1102-15.
32. Posselt, D., *Eisen(diarylsalen)-Komplexe als neuartige Zytostatika: Synthese, pharmakologische und biochemische Untersuchungen zum Wirkungsmechanismus, Dissertation, in Fachbereich Biologie, Chemie, Pharmazie.* 2006, Freie Universität Berlin.
33. Peter C. Heinrich, Matthias Müller, and L. Graeve, *Löffler/Petrides Biochemie und Pathobiochemie.* Vol. 9. 2014: Springer-Verlag Berlin Heidelberg.
34. Weisiger, R.A. and I. Fridovich, *Mitochondrial superoxide dismutase: site of synthesis and intramitochondrial localization.* J Biol Chem, 1973. **248**: p. 4793-4796.
35. Murphy M , P., *How mitochondria produce reactive oxygen species.* Biochem J, 2009. **417**(Pt 1): p. 1-13.
36. Gottlieb, R.A., *Cytochrome P450: major player in reperfusion injury.* Arch Biochem Biophys, 2003. **420**(2): p. 262-7.
37. Holmstrom, K.M. and T. Finkel, *Cellular mechanisms and physiological consequences of redox-dependent signalling.* Nat Rev Mol Cell Biol, 2014. **15**(6): p. 411-21.
38. Sies, H., *Role of Metabolic H2O2 Generation: REDOX SIGNALING AND OXIDATIVE STRESS.* Journal of Biological Chemistry, 2014. **289**(13): p. 8735-8741.
39. Yada, T., et al., *Hydrogen Peroxide, an Endogenous Endothelium-Derived Hyperpolarizing Factor, Plays an Important Role in Coronary Autoregulation In Vivo.* Circulation, 2003. **107**(7): p. 1040-1045.
40. Lange, A., *Die NO/cGMP-vermittelte Signaltransduktion in der glatten Muskulatur, Inauguraldissertation, in Fakultät für Medizin.* 2006, Ruhr-Universität Bochum.
41. Merx, M.W., et al., *Depletion of circulating blood NOS3 increases severity of myocardial infarction and left ventricular dysfunction.* Basic Res Cardiol, 2014. **109**(1): p. 398.
42. Cortese-Krott, M.M. and M. Kelm, *Endothelial nitric oxide synthase in red blood cells: key to a new erythrocrine function? Redox Biol, 2014. 2: p. 251-8.*

43. Kostic, M.M. and J. Schrader, *Role of nitric oxide in reactive hyperemia of the guinea pig heart*. *Circ Res*, 1992. **70**(1): p. 208-12.
44. Godecke, A., et al., *Coronary hemodynamics in endothelial NO synthase knockout mice*. *Circ Res*, 1998. **82**(2): p. 186-94.
45. Balligand, J.L., O. Feron, and C. Dessy, *eNOS activation by physical forces: from short-term regulation of contraction to chronic remodeling of cardiovascular tissues*. *Physiol Rev*, 2009. **89**(2): p. 481-534.
46. Fleming, I., *Molecular mechanisms underlying the activation of eNOS*. *Pflugers Arch*, 2010. **459**(6): p. 793-806.
47. Heiss, C., A. Rodriguez-Mateos, and M. Kelm, *Central role of eNOS in the maintenance of endothelial homeostasis*. *Antioxid Redox Signal*, 2015. **22**(14): p. 1230-42.
48. Gorrini, C., I.S. Harris, and T.W. Mak, *Modulation of oxidative stress as an anticancer strategy*. *Nat Rev Drug Discov*, 2013. **12**(12): p. 931-947.
49. Harman, D., *Aging: a theory based on free radical and radiation chemistry*. *J Gerontol*, 1956. **11**(3): p. 298-300.
50. Zhang, H., K.J. Davies, and H.J. Forman, *Oxidative stress response and Nrf2 signaling in aging*. *Free Radic Biol Med*, 2015.
51. Sohal, R.S. and W.C. Orr, *The redox stress hypothesis of aging*. *Free Radical Biology and Medicine*, 2012. **52**(3): p. 539-555.
52. Stuart, J.A., et al., *A midlife crisis for the mitochondrial free radical theory of aging*. *Longevity & Healthspan*, 2014. **3**(1): p. 1-15.
53. Sussan, T.E., et al., *Disruption of Nrf2, a Key Inducer of Antioxidant Defenses, Attenuates ApoE-Mediated Atherosclerosis in Mice*. *PLoS ONE*, 2008. **3**(11): p. e3791.
54. Ungvari, Z., et al., *Age-associated vascular oxidative stress, Nrf2 dysfunction, and NF- κ B activation in the nonhuman primate *Macaca mulatta**. *J Gerontol A Biol Sci Med Sci*, 2011. **66**(8): p. 866-75.
55. Chen, B., et al., *The role of Nrf2 in oxidative stress-induced endothelial injuries*. *J Endocrinol*, 2015. **225**(3): p. R83-99.
56. Babusikova, E., et al., *Age-associated changes in Ca(2+)-ATPase and oxidative damage in sarcoplasmic reticulum of rat heart*. *Physiol Res*, 2012. **61**(5): p. 453-60.
57. Wu, J., et al., *The Role of Oxidative Stress and Inflammation in Cardiovascular Aging*. 2014. **2014**: p. 615312.
58. Jaiswal, A.K., *Antioxidant response element*. *Biochem Pharmacol*, 1994. **48**(3): p. 439-44.
59. Niture, S.K., et al., *Nrf2 signaling and cell survival*. *Toxicol Appl Pharmacol*, 2010. **244**(1): p. 37-42.
60. Nguyen, T., H.C. Huang, and C.B. Pickett, *Transcriptional regulation of the antioxidant response element. Activation by Nrf2 and repression by MafK*. *J Biol Chem*, 2000. **275**(20): p. 15466-73.
61. Nguyen, T., P.J. Sherratt, and C.B. Pickett, *Regulatory mechanisms controlling gene expression mediated by the antioxidant response element*. *Annu Rev Pharmacol Toxicol*, 2003. **43**: p. 233-60.
62. Nguyen, T., C.S. Yang, and C.B. Pickett, *The pathways and molecular mechanisms regulating Nrf2 activation in response to chemical stress*. *Free Radic Biol Med*, 2004. **37**(4): p. 433-41.
63. Nguyen, T., P. Nioi, and C.B. Pickett, *The Nrf2-antioxidant response element signaling pathway and its activation by oxidative stress*. *J Biol Chem*, 2009. **284**(20): p. 13291-5.
64. Niture, S.K., R. Khatri, and A.K. Jaiswal, *Regulation of Nrf2—an update*. *Free Radical Biology and Medicine*, 2014. **66**(0): p. 36-44.

65. Kaspar, J.W., S.K. Niture, and A.K. Jaiswal, *Nrf2:INrf2 (Keap1) signaling in oxidative stress*. *Free Radic Biol Med*, 2009. **47**(9): p. 1304-9.
66. Owuor, E.D. and A.N. Kong, *Antioxidants and oxidants regulated signal transduction pathways*. *Biochem Pharmacol*, 2002. **64**(5-6): p. 765-70.
67. Aggarwal, N.T. and J.C. Makielski, *Redox control of cardiac excitability*. *Antioxid Redox Signal*, 2013. **18**(4): p. 432-68.
68. Lippross, S., et al., *Nrf2 deficiency impairs fracture healing in mice*. *Calcif Tissue Int*, 2014. **95**(4): p. 349-61.
69. Pearson, K.J., et al., *Nrf2 mediates cancer protection but not longevity induced by caloric restriction*. *Proceedings of the National Academy of Sciences*, 2008. **105**(7): p. 2325-2330.
70. Jiang, T., et al., *The Protective Role of Nrf2 in Streptozotocin-Induced Diabetic Nephropathy*. *Diabetes*, 2010. **59**(4): p. 850-860.
71. de Vries, H.E., et al., *Nrf2-induced antioxidant protection: a promising target to counteract ROS-mediated damage in neurodegenerative disease?* *Free Radic Biol Med*, 2008. **45**(10): p. 1375-83.
72. Li, J., et al., *Nrf2 protects against maladaptive cardiac responses to hemodynamic stress*. *Arterioscler Thromb Vasc Biol*, 2009. **29**(11): p. 1843-50.
73. Li, J., et al., *Up-regulation of p27(kip1) contributes to Nrf2-mediated protection against angiotensin II-induced cardiac hypertrophy*. *Cardiovasc Res*, 2011. **90**(2): p. 315-24.
74. Barajas, B., et al., *NF-E2-Related Factor 2 Promotes Atherosclerosis by Effects on Plasma Lipoproteins and Cholesterol Transport That Overshadow Antioxidant Protection*. *Arteriosclerosis, Thrombosis, and Vascular Biology*, 2011. **31**(1): p. 58-66.
75. Kuang, L., et al., *Knockdown of Nrf2 inhibits the angiogenesis of rat cardiac microvascular endothelial cells under hypoxic conditions*. *Int J Biol Sci*, 2013. **9**(7): p. 656-65.
76. Van-Assche, T., et al., *Gene therapy targeting inflammation in atherosclerosis*. *Curr Pharm Des*, 2011. **17**(37): p. 4210-23.
77. Zakkar, M., et al., *Activation of Nrf2 in endothelial cells protects arteries from exhibiting a proinflammatory state*. *Arterioscler Thromb Vasc Biol*, 2009. **29**(11): p. 1851-7.
78. Zhu, H., et al., *Antioxidants and phase 2 enzymes in macrophages: regulation by Nrf2 signaling and protection against oxidative and electrophilic stress*. *Exp Biol Med (Maywood)*, 2008. **233**(4): p. 463-74.
79. Liu, T.-s., et al., *Oscillating high glucose enhances oxidative stress and apoptosis in human coronary artery endothelial cells*. *Journal of Endocrinological Investigation*, 2014. **37**(7): p. 645-651.
80. Ungvari, Z., et al., *Adaptive induction of NF-E2-related factor-2-driven antioxidant genes in endothelial cells in response to hyperglycemia*. *American Journal of Physiology - Heart and Circulatory Physiology*, 2011. **300**(4): p. H1133-H1140.
81. Eba, S., et al., *The nuclear factor erythroid 2-related factor 2 activator oltipraz attenuates chronic hypoxia-induced cardiopulmonary alterations in mice*. *Am J Respir Cell Mol Biol*, 2013. **49**(2): p. 324-33.
82. Qu, C., et al., *Identifying panaxynol, a natural activator of nuclear factor erythroid-2 related factor 2 (Nrf2) from American ginseng as a suppressor of inflamed macrophage-induced cardiomyocyte hypertrophy*. *Journal of Ethnopharmacology*, 2015. **168**: p. 326-336.
83. Suh, J.H., et al., *Decline in transcriptional activity of Nrf2 causes age-related loss of glutathione synthesis, which is reversible with lipoic acid*. *Proc Natl Acad Sci U S A*, 2004. **101**(10): p. 3381-6.
84. Jasper, H., *SKNy Worms and Long Life*. *Cell*, 2008. **132**(6): p. 915-916.

85. Wu, S., et al., *Cardiac-specific overexpression of catalase prolongs lifespan and attenuates ageing-induced cardiomyocyte contractile dysfunction and protein damage*. Clin Exp Pharmacol Physiol, 2007. **34**(1-2): p. 81-7.
86. Hoshino, T., et al., *Protective role of Nrf2 in age-related hearing loss and gentamicin ototoxicity*. Biochemical and Biophysical Research Communications, 2011. **415**(1): p. 94-98.
87. Gargiulo, S., et al., *Mice anesthesia, analgesia, and care, Part I: anesthetic considerations in preclinical research*. Ilar j, 2012. **53**(1): p. E55-69.
88. Kober, F., et al., *Myocardial blood flow mapping in mice using high-resolution spin labeling magnetic resonance imaging: influence of ketamine/xylazine and isoflurane anesthesia*. Magn Reson Med, 2005. **53**(3): p. 601-6.
89. Hart, C.Y., J.C. Burnett, Jr., and M.M. Redfield, *Effects of avertin versus xylazine-ketamine anesthesia on cardiac function in normal mice*. Am J Physiol Heart Circ Physiol, 2001. **281**(5): p. H1938-45.
90. Xu, Q., et al., *Optimizing dosage of ketamine and xylazine in murine echocardiography*. Clin Exp Pharmacol Physiol, 2007. **34**(5-6): p. 499-507.
91. Pacher, P., et al., *Measurement of cardiac function using pressure-volume conductance catheter technique in mice and rats*. Nat Protoc, 2008. **3**(9): p. 1422-34.
92. Bell, R.M., M.M. Mocanu, and D.M. Yellon, *Retrograde heart perfusion: the Langendorff technique of isolated heart perfusion*. J Mol Cell Cardiol, 2011. **50**(6): p. 940-50.
93. Skrzypiec-Spring, M., et al., *Isolated heart perfusion according to Langendorff---still viable in the new millennium*. J Pharmacol Toxicol Methods, 2007. **55**(2): p. 113-26.
94. HUGO SACHS ELEKTRONIK and HARVARD APPARATUS GmbH, *Operating Instructions for the ISOLATED HEART FOR SMALL RODENTS IH-SR, Type 844 (Version 2.1)*. 2010. p. 14-16.
95. Feldman, A.M., et al., *Adenosine receptor subtypes and the heart failure phenotype: translating lessons from mice to man*. Trans Am Clin Climatol Assoc, 2011. **122**: p. 198-214.
96. Berne, R.M., *Cardiac nucleotides in hypoxia: possible role in regulation of coronary blood flow*. American Journal of Physiology -- Legacy Content, 1963. **204**(2): p. 317-322.
97. Deussen, A., et al., *Metabolic coronary flow regulation--current concepts*. Basic Res Cardiol, 2006. **101**(6): p. 453-64.
98. Belardinelli, L., et al., *The A2A adenosine receptor mediates coronary vasodilation*. J Pharmacol Exp Ther, 1998. **284**(3): p. 1066-73.
99. Flood, A. and J.P. Headrick, *Functional characterization of coronary vascular adenosine receptors in the mouse*. Br J Pharmacol, 2001. **133**(7): p. 1063-72.
100. Li, J., et al., *Adenosine A2a receptors increase arterial endothelial cell nitric oxide*. J Surg Res, 1998. **80**(2): p. 357-64.
101. Sharifi-Sanjani, M., et al., *Interactions between A2A adenosine receptors, hydrogen peroxide, and KATP channels in coronary reactive hyperemia*. Vol. 304. 2013. H1294-H1301.
102. Zhou, X., et al., *A1 adenosine receptor negatively modulates coronary reactive hyperemia via counteracting A2A-mediated H2O2 production and KATP opening in isolated mouse hearts*. Am J Physiol Heart Circ Physiol, 2013. **305**(11): p. H1668-79.
103. Zhou, Z., et al., *Involvement of NADPH oxidase in A2A adenosine receptor-mediated increase in coronary flow in isolated mouse hearts*. Purinergic Signal, 2015. **11**(2): p. 263-73.

104. El-Awady, M.S., et al., *Evidence for the involvement of NADPH oxidase in adenosine receptors-mediated control of coronary flow using A and A knockout mice*. *Physiol Rep*, 2013. **1**(3): p. e00070.
105. Saitoh, S., et al., *Hydrogen peroxide: a feed-forward dilator that couples myocardial metabolism to coronary blood flow*. *Arterioscler Thromb Vasc Biol*, 2006. **26**(12): p. 2614-21.
106. Maurer, M., et al., *New topics in bradykinin research*. *Allergy*, 2011. **66**(11): p. 1397-406.
107. Dumoulin, M.J., et al., *Metabolism of bradykinin by the rat coronary vascular bed*. *Cardiovasc Res*, 1998. **38**(1): p. 229-36.
108. Su, J.B., et al., *Stimulation of bradykinin B(1) receptors induces vasodilation in conductance and resistance coronary vessels in conscious dogs: comparison with B(2) receptor stimulation*. *Circulation*, 2000. **101**(15): p. 1848-53.
109. Pelc, L.R., G.J. Gross, and D.C. Warltier, *Mechanism of coronary vasodilation produced by bradykinin*. *Circulation*, 1991. **83**(6): p. 2048-56.
110. Larsen, B.T., et al., *Bradykinin-induced dilation of human coronary arterioles requires NADPH oxidase-derived reactive oxygen species*. *Arterioscler Thromb Vasc Biol*, 2009. **29**(5): p. 739-45.
111. Cowan, C.L. and R.A. Cohen, *Two mechanisms mediate relaxation by bradykinin of pig coronary artery: NO-dependent and -independent responses*. *Am J Physiol*, 1991. **261**(3 Pt 2): p. H830-5.
112. Kuga, T., et al., *Bradykinin-induced vasodilation of human coronary arteries in vivo: role of nitric oxide and angiotensin-converting enzyme*. *J Am Coll Cardiol*, 1997. **30**(1): p. 108-12.
113. Böhm, M. and A.T. Bäumer, *Referenz-Reihe Kardiologie Herzinsuffizienz*. 2000, Stuttgart: Georg Thieme Verlag.
114. Joachim Rassow, et al., *Duale Reihe Biochemie*. Vol. 3. 2012, Stuttgart: Georg Thieme Verlag.
115. Fürstenwerth, H., *Ouabain – the insulin of the heart*. *International Journal of Clinical Practice*, 2010. **64**(12): p. 1591-1594.
116. Ziff, O.J., et al., *Safety and efficacy of digoxin: systematic review and meta-analysis of observational and controlled trial data*. *Bmj*, 2015. **351**: p. h4451.
117. Lewis, L.K., et al., *Endogenous Ouabain Is Not Ouabain*. *Hypertension*, 2014. **64**(4): p. 680-683.
118. Yoh, K., et al., *Nrf2-deficient female mice develop lupus-like autoimmune nephritis*. *Kidney Int*, 2001. **60**(4): p. 1343-53.
119. Lorenz, J.N., *A practical guide to evaluating cardiovascular, renal, and pulmonary function in mice*. *Am J Physiol Regul Integr Comp Physiol*, 2002. **282**(6): p. R1565-82.
120. Kristian, T. and B. Hu, *Guidelines for using mouse global cerebral ischemia models*. *Transl Stroke Res*, 2013. **4**(3): p. 343-50.
121. Fujii, M., et al., *Strain-related differences in susceptibility to transient forebrain ischemia in SV-129 and C57black/6 mice*. *Stroke*, 1997. **28**(9): p. 1805-11.
122. Fleenor, B.S., et al., *Superoxide signaling in perivascular adipose tissue promotes age-related artery stiffness*. *Aging Cell*, 2014. **13**(3): p. 576-8.
123. Fleenor, B.S., et al., *Superoxide-lowering therapy with TEMPOL reverses arterial dysfunction with aging in mice*. *Aging Cell*, 2012. **11**(2): p. 269-76.
124. Sag, C.M., et al., *Ionizing radiation regulates cardiac Ca handling via increased ROS and activated CaMKII*. *Basic Res Cardiol*, 2013. **108**(6): p. 385.
125. Csordás, G. and G. Hajnóczy, *SR/ER-mitochondrial local communication: Calcium and ROS*. *Biochim Biophys Acta*, 2009. **1787**(11): p. 1352-62.

126. Periasamy, M., P. Bhupathy, and G.J. Babu, *Regulation of sarcoplasmic reticulum Ca²⁺ ATPase pump expression and its relevance to cardiac muscle physiology and pathology*. Cardiovascular Research, 2008. **77**(2): p. 265-273.
127. Lompré, A.-M., M. Anger, and D. Levitsky, *Sarco(endo)plasmic Reticulum Calcium Pumps in the Cardiovascular System: Function and Gene Expression*. Journal of Molecular and Cellular Cardiology, 1994. **26**(9): p. 1109-1121.
128. Tsai, C.T., et al., *TNF-alpha down-regulates sarcoplasmic reticulum Ca(2+)-ATPase expression and leads to left ventricular diastolic dysfunction through binding of NF-kappaB to promoter response element*. Cardiovasc Res, 2015. **105**(3): p. 318-29.
129. Jiang, M.T., M.P. Moffat, and N. Narayanan, *Age-related alterations in the phosphorylation of sarcoplasmic reticulum and myofibrillar proteins and diminished contractile response to isoproterenol in intact rat ventricle*. Circulation Research, 1993. **72**(1): p. 102-11.
130. Lakatta, E.G. and S.J. Sollott, *Perspectives on mammalian cardiovascular aging: humans to molecules*. Comp Biochem Physiol A Mol Integr Physiol, 2002. **132**(4): p. 699-721.
131. Jiao, Q., et al., *Sarcolumenin plays a critical role in age-related cardiac dysfunction due to decreases in SERCA2a expression and activity*. Cell Calcium, 2012. **51**(1): p. 31-9.
132. Lim, C.C., et al., *Impaired lusitropy-frequency in the aging mouse: role of Ca(2+)-handling proteins and effects of isoproterenol*. Am J Physiol, 1999. **277**(5 Pt 2): p. H2083-90.
133. Rueckschloss, U., M. Villmow, and U. Klöckner, *NADPH oxidase-derived superoxide impairs calcium transients and contraction in aged murine ventricular myocytes*. Experimental Gerontology, 2010. **45**(10): p. 788-796.
134. Ren, J., et al., *Cardiac overexpression of antioxidant catalase attenuates aging-induced cardiomyocyte relaxation dysfunction*. Mech Ageing Dev, 2007. **128**(3): p. 276-85.
135. Dai, D.F., et al., *Overexpression of catalase targeted to mitochondria attenuates murine cardiac aging*. Circulation, 2009. **119**(21): p. 2789-97.
136. Qin, F., et al., *Hydrogen peroxide-mediated SERCA cysteine 674 oxidation contributes to impaired cardiac myocyte relaxation in senescent mouse heart*. J Am Heart Assoc, 2013. **2**(4): p. e000184.
137. Kubin, A.M., et al., *Role of reactive oxygen species in the regulation of cardiac contractility*. J Mol Cell Cardiol, 2011. **50**(5): p. 884-93.
138. Brennan, J.P., et al., *Oxidant-induced activation of type I protein kinase A is mediated by RI subunit interprotein disulfide bond formation*. J Biol Chem, 2006. **281**(31): p. 21827-36.
139. Viola, H.M., P.G. Arthur, and L.C. Hool, *Transient exposure to hydrogen peroxide causes an increase in mitochondria-derived superoxide as a result of sustained alteration in L-type Ca²⁺ channel function in the absence of apoptosis in ventricular myocytes*. Circ Res, 2007. **100**(7): p. 1036-44.
140. Johnstone, V.P. and L.C. Hool, *Glutathionylation of the L-type Ca²⁺ channel in oxidative stress-induced pathology of the heart*. Int J Mol Sci, 2014. **15**(10): p. 19203-25.
141. Carnes, C.A., et al., *Atrial glutathione content, calcium current, and contractility*. J Biol Chem, 2007. **282**(38): p. 28063-73.
142. Sumandea, M.P. and S.F. Steinberg, *Redox signaling and cardiac sarcomeres*. J Biol Chem, 2011. **286**(12): p. 9921-7.
143. Feridooni, H.A., K.M. Dibb, and S.E. Howlett, *How cardiomyocyte excitation, calcium release and contraction become altered with age*. J Mol Cell Cardiol, 2015. **83**: p. 62-72.
144. Csiszar, A., et al., *Aging-induced phenotypic changes and oxidative stress impair coronary arteriolar function*. Circ Res, 2002. **90**(11): p. 1159-66.

145. Marczak, E.D., et al., *Polymorphisms in the transcription factor NRF2 and forearm vasodilator responses in humans*. *Pharmacogenet Genomics*, 2012. **22**(8): p. 620-8.
146. Heiss, E.H., et al., *Active NF-E2-related factor (Nrf2) contributes to keep endothelial NO synthase (eNOS) in the coupled state: role of reactive oxygen species (ROS), eNOS, and heme oxygenase (HO-1) levels*. *J Biol Chem*, 2009. **284**(46): p. 31579-86.
147. Lauer, N., et al., *Critical involvement of hydrogen peroxide in exercise-induced up-regulation of endothelial NO synthase*. Vol. 65. 2005. 254-262.
148. Drummond, G.R., et al., *Transcriptional and Posttranscriptional Regulation of Endothelial Nitric Oxide Synthase Expression by Hydrogen Peroxide*. *Circulation Research*, 2000. **86**(3): p. 347-354.
149. Cai, H., et al., *Induction of Endothelial NO Synthase by Hydrogen Peroxide via a Ca²⁺/Calmodulin-Dependent Protein Kinase II/Janus Kinase 2-Dependent Pathway*. *Arteriosclerosis, Thrombosis, and Vascular Biology*, 2001. **21**(10): p. 1571-1576.
150. Hool, L.C., *What cardiologists should know about calcium ion channels and their regulation by reactive oxygen species*. *Heart Lung Circ*, 2007. **16**(5): p. 361-72.
151. Rigolli, M. and G.A. Whalley, *Heart failure with preserved ejection fraction*. *J Geriatr Cardiol*, 2013. **10**(4): p. 369-76.

Acknowledgement

Auch wenn diese Arbeit mein eigenes Werk ist, so gibt es doch eine ganze Reihe an Personen, die daran beteiligt waren. Darum danke ich dem gesamten kardiologischen Forschungsteam der Uni Düsseldorf. Auch wenn ich an dieser Stelle nur wenige namentlich nennen kann, so war es mir doch eine Ehre mit Euch allen zu arbeiten und zu forschen.

Mein besonderer Dank gilt Frau Prof. Dr. rer. nat. Dr. Miriam M. Cortese-Krott für ihre Unterstützung und Betreuung, für ihr stetiges Interesse an meiner Arbeit und ihre konstruktive Kritik. Danke auch für die Möglichkeit der Präsentation meiner Ergebnisse auf der 80. Jahrestagung der Deutschen Gesellschaft für Kardiologie 2014 in Mannheim. Ohne ihre Hilfe wäre diese Arbeit nicht möglich gewesen.

Ein großer Dank gilt auch Herrn Professor Dr. med. Malte Kelm, Direktor der Klinik für Kardiologie, Pneumologie und Angiologie, für die zur Verfügung gestellten Mittel, sowie für sein Interesse an meiner Arbeit.

Vielen Dank an Dr. med. Ralf Erkens für die kritische Auseinandersetzung mit den Echokardiographie-Daten, sowie der zahlreichen Anregungen für die Dissertation. Ich danke auch Dr. rer. nat. Thomas Krenz, der mir grade zu Beginn ein stetiger Ansprechpartner und eine große Hilfe war. Dasselbe gilt natürlich auch für Stefanie Becher. Unzählige Male habe ich sie mit Fragen gelöchert und Problemen konfrontiert, welche sie stets mit Hilfe ihrer immensen Erfahrung lösen konnte.

Ich danke Herrn Professor Dr. rer. nat. Axel Gödecke und dem Team des Instituts für Herz- und Kreislaufphysiologie, für die Mitbenutzung Ihres Labors. Vielen Dank auch an Herrn Thomas Beha von der Firma Hugo-Sachs Elektronik, Harvard Apparatus GmbH, für die freundlicher Weise zur Verfügung gestellte Langendorff Konstruktionszeichnung.

Zu guter Letzt besonderer Dank an die anderen Doktoranden für die gute Musik, die vielen Witze und die lustige Zeit. Forschung muss ja nicht immer nur ernst sein.